REVIEWS OF GEOPHYSICS VOL. 6, NO. 3 AUGUST 1968

Rapid Estimation of the Topographic Disturbance to Superficial Thermal Gradients[1]

ARTHUR H. LACHENBRUCH

U. S. Geological Survey, Menlo Park, California

Abstract. The Jeffreys-Bullard theory of the topographic correction to geothermal gradients cannot be applied with confidence if the height of the relief is large relative to the horizontal distance and depth of the measurement points. It cannot be generally applied to shallow probe measurements in the ocean bottom if bold relief occurs on a scale exceeding a few meters, or on continents to observation in shallow boreholes in extremely rugged terrain.

In an important special case, where the measurement depth is small relative to the distance to the relief, the 'superficial' gradient anomaly may be approximated by the value applicable at zero depth. A fairly general two-dimensional steady-state theory for this case can be based on the solution for heat flux through an inclined plane of arbitrary height and slope angle. These two parameters are easily visualized and represented graphically so that models which approximate or bracket real topography can be identified quickly. The results can be applied to stations on planes, valleys, ridges, or benches bounded by irregular slopes. They are valid for points arbitrarily close to slopes of any height or inclination. Finite slope and curvature of the surface at the station can be accommodated if they are not too great. Even if other theories of the topographic correction are applicable, the present method can be useful, as it leads to rapid estimates by graphical means and to useful limits even if the superficial condition is not satisfied.

Curvature in an ocean-bottom temperature profile justifies suspicion of a topographic disturbance from undetected relief. The temperature probe's length should be 2 or 3 times the uncertainty in local elevation difference, and measured curvature should be negligible for reasonable assurance that undetected relief is not causing gradient errors greater than ±10%. Relief not detectable with conventional echo sounders, but of the type observed with deeply towed sounding equipment, can cause heat-flow anomalies of 50–100%, and relatively little curvature will be indicated by probes a few meters long. The very high oceanic heat flows are difficult to explain by undetected relief, but the very low ones are not.

1. INTRODUCTION

The pattern of heat flow from the earth's deep interior is distorted near the surface by topographic relief; the flux is intensified by valleys and attenuated by ridges. To obtain regionally significant heat-flow values in areas with appreciable relief, we must correct for these effects.

Traditionally the theory of the geothermal topographic correction has been approached in two different ways [*Jaeger,* 1965, section 5]: In the first [*Jeffreys,* 1938; *Bullard,* 1938; *Birch,* 1950], a fundamental mathematical simplification

[1] Publication authorized by the Director, U. S. Geological Survey.

results from replacing the irregular surface by a horizontal reference plane upon which the temperature varies in proportion to the relative elevation of the actual surface. Interaction between the topographic features is thus neglected, and the independent effects of elements of the topography can be summed to obtain the approximate correction. There is no limit to the fidelity with which the topographic surface can be represented, as the representation is achieved with a numerical procedure.

In the second approach (applied most recently by *Birch* [1967] and *Jaeger and Sass* [1963]), the true surface is approximated by a simple geometric surface and its effects on the gradient are computed directly. Thus the second approach yields the exact effects of an approximate representation of topography, and the first yields the approximate effects of an (effectively) exact representation of topography.

As *Birch* [1950] has shown, the first method is more general, and it lends itself readily to refinements accounting for topographic evolution. It has been pointed out by *Jaeger and Sass* [1963] that the second method is useful for very rapid estimates of terrain effects if detailed corrections are not warranted because of imperfectly known topography or other uncertain sources of disturbance. The last statement depends upon the geometric model being sufficiently simple to be easily identified with the topographic surface to be approximated. Both methods generally become less satisfactory as the gradient measurement to be corrected approaches the surface. This can be explained as follows: In general, the frequency of occurrence of features of the earth's topographic relief decreases as the size of the feature increases; the largest and most infrequent features have a vertical scale of the order of a few kilometers. However, the effect of topographic features on the geothermal gradient is not large as long as their height is (1) less than the horizontal distance to the measurement point or (2) less than the depth of measurement. Thus, for measurements a few kilometers beneath the surface, condition 2 is satisfied, even for the most rugged relief (at any horizontal distance); a gross representation of the topography, used with any reasonable approximation scheme, will generally suffice. As the measurement points approach the surface, progressively smaller (and more frequently occurring) features will fail to satisfy condition 2, and those that are not far enough from the station to satisfy condition 1 will have to be accounted for with progressively increasing rigor; although the effects of distant relief do not diminish, the effects of close-in relief increase greatly, and small-scale irregularities can cause sizable anomalies. Under these conditions the second method becomes less satisfactory because it becomes increasingly difficult to represent close-in relief in detail and still account for distant relief in a gross way with a simple geometrical model. The first method becomes uncertain for near-surface measurements because it neglects second-order effects arising from lateral variations of the vertical gradient in the relief. These effects can become appreciable when close-in relief must be considered. *Birch* [1950, p. 625] pointed out that 'at shallow depths, under sharp irregularities, the approximation is sure to be poor.'

Observations of earth heat flow made to date can be grouped into two rather

distinct categories: continental and oceanic. Continental measurements (representing about 10% of the values according to *Lee and Uyeda* [1965]) are made to depths of the order of a kilometer beneath the land surface. The relief is observable and can be considered known. Oceanic measurements account for the remaining 90% of the observations. They are made to depths of only a few meters beneath the sea floor, and the pertinent relief must be considered largely unknown. On the continents it is often possible to select measurement sites at places where the topographic disturbance is small, and an approximate theory can be used with confidence. In the oceans, however, unseen relief might cause very large errors. Attempts to estimate how large these errors might be can be misleading if they are based on an approximate mathematical theory.

In most observational studies of earth heat flow, continental or oceanic, it is usually found that for every calculation of a detailed topographic correction, many rough calculations are made to determine whether a given feature is significant, or to determine the order of magnitude of its contribution. For this purpose there seems to be some use for results from an extemely simple geometric model that can be applied without regard for the validity of any mathematical approximation. This problem is considered in the present paper.

The starting point is the exact solution for the gradient disturbance at the surface caused by the simplest topographic form, an inclined plane segment of angle β, joining horizontal half planes with elevation difference H. The geometry is two-dimensional, and the medium is assumed to be homogeneous and in a thermal steady state. In return for this loss of generality we gain the advantage of two-parameter representation of results in simple graphical form. These parameters, slope angle and slope height, are so easily visualized that models which might bracket or approximate real topography can be identified quickly. The results apply directly only to 'superficial gradient measurements,' which we define as those for which the topographic correction can be approximated well by the value applicable at the surface. Hence they concern measurements to depths that are less than the horizontal distance to the relief, but the height of the relief may be arbitrarily large. They therefore apply to many cases (particularly in oceanic applications) for which the standard Jeffreys approximation is quite uncertain. The results also yield limits for cases in which the superficial condition is not satisfied.

The plan of this paper is as follows. The next section presents numerical results for the exact solution just discussed, and section 3 compares them with the corresponding results obtained from the Jeffreys reference-plane assumption. Section 4 gives upper and lower limits for the surface heat flow where two slopes co-exist to form a 'plane valley,' 'plane ridge,' or 'plane bench.' In section 5, a simple procedure is described for bracketing the anomaly due to a general slope with exact results for plane slopes. Section 6 combines the first and second approaches to terrain corrections (described in the previous paragraphs) to obtain a method for approximating and bracketing the effects of a general slope, and conversely gives conditions under which a general slope can be represented by a plane slope. In section 7, conditions for neglecting gentle slopes at the station are presented, and the variation of the topographic anomaly with depth

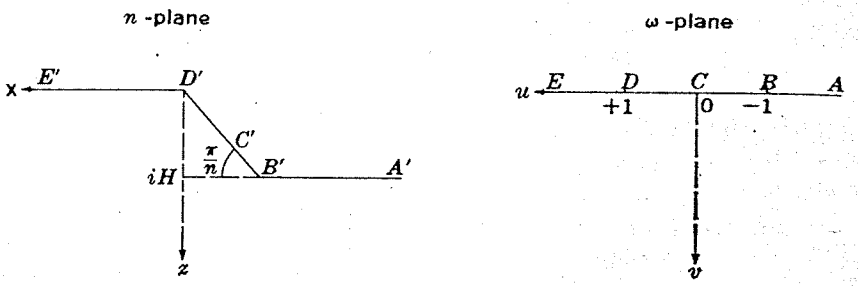

Fig. 1. Transformation of the plane boundary of a half-space into a plane slope.

and the conditions under which a gradient anomaly may be considered superficial are discussed in section 8. Transient effects and an additional application of the results of section 2, the heat-flow anomaly caused by a down-faulted bedrock pediment, are considered in section 9.

I intend to present results in usable graphical and tabular form and to provide some insight into the quantitative behavior of the superficial gradient disturbance. For brevity, the mathematical results are generally presented without derivation. In some cases they are eliminated altogether, and results are shown only in graphical form. For additional discussion and justification of these results, the reader is referred to *Lachenbruch* [1968]. That work will be designated in the text by the abbreviation *TDT* (Two-Dimensional Topography).

2. HEAT FLOW THROUGH A PLANE SLOPE: EXACT SOLUTION

An expression is needed for the vertical thermal flux through a plane slope on the earth's surface. The earth is assumed to be homogeneous and isotropic, and the surface is represented by a plane segment inclined at an angle β to horizontal surfaces beyond the toe and behind the brink which are at an elevation difference H. The model is illustrated by the region below the contour Γ' ($A'B'C'D'E'$) in the η plane, Figure 1. The slope angle β is represented by π/n. To represent otherwise uniform conditions, it is assumed that the surface (Γ') is at zero temperature and that at large distances from the slope the temperature is proportional to distance beneath the surface.

The special case of the vertical cliff ($n = 2$) has been discussed by *Castoldi* [1952]. His solution was obtained by mapping a uniform field in the ω plane into the region bounded by a step-shaped contour of the η plane with the conformal transformation

$$\frac{d\eta}{d\omega} = A\left(\frac{\omega + 1}{\omega - 1}\right)^{1/2}$$

The more general function [*Kober*, 1952, p. 161]

$$\frac{d\eta}{d\omega} = A\left(\frac{\omega + 1}{\omega - 1}\right)^{1/n}, \; n \text{ a positive integer} \tag{1}$$

achieves the mapping illustrated in Figure 1.

The vertical gradient of temperature at the contour Γ' (a plane slope) can be obtained by a contour integration. The resulting equations are too cumbersome to yield insight by inspection, and they will not be reproduced here (see *TDT*, section 2).

The following notation is used in the presentation of numerical results:

$G = Q/K$, where Q is the regional heat flux, K is the thermal conductivity, and G is the regional thermal gradient.

$(K/Q)(\partial\Theta/\partial z) = q$, where θ is temperature in the earth and q is normalized vertical heat flux at surface (Γ').

s, distance behind brink (i.e., to the left from D', Figure 1) in units of slope height.

r, distance beyond toe (i.e., to the right from B', Figure 1) in units of slope height.

w, horizontal distance from brink (to the right from D', Figure 1) in units of slope width.

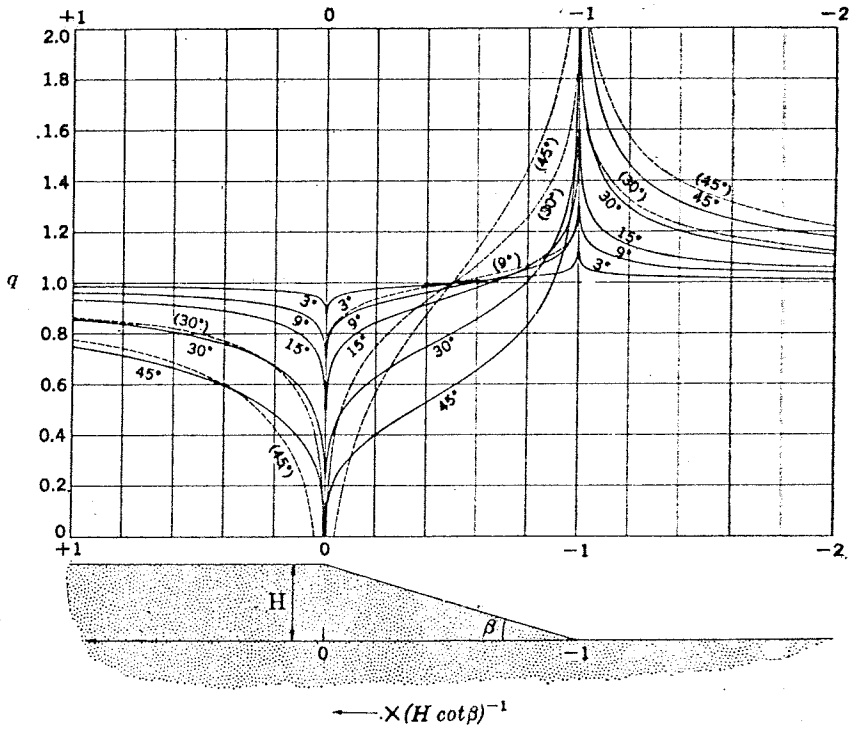

Fig. 2. Vertical component of normalized heat flow through a plane slope. Solid curves represent exact results; dashed curves represent the Jeffreys approximation.

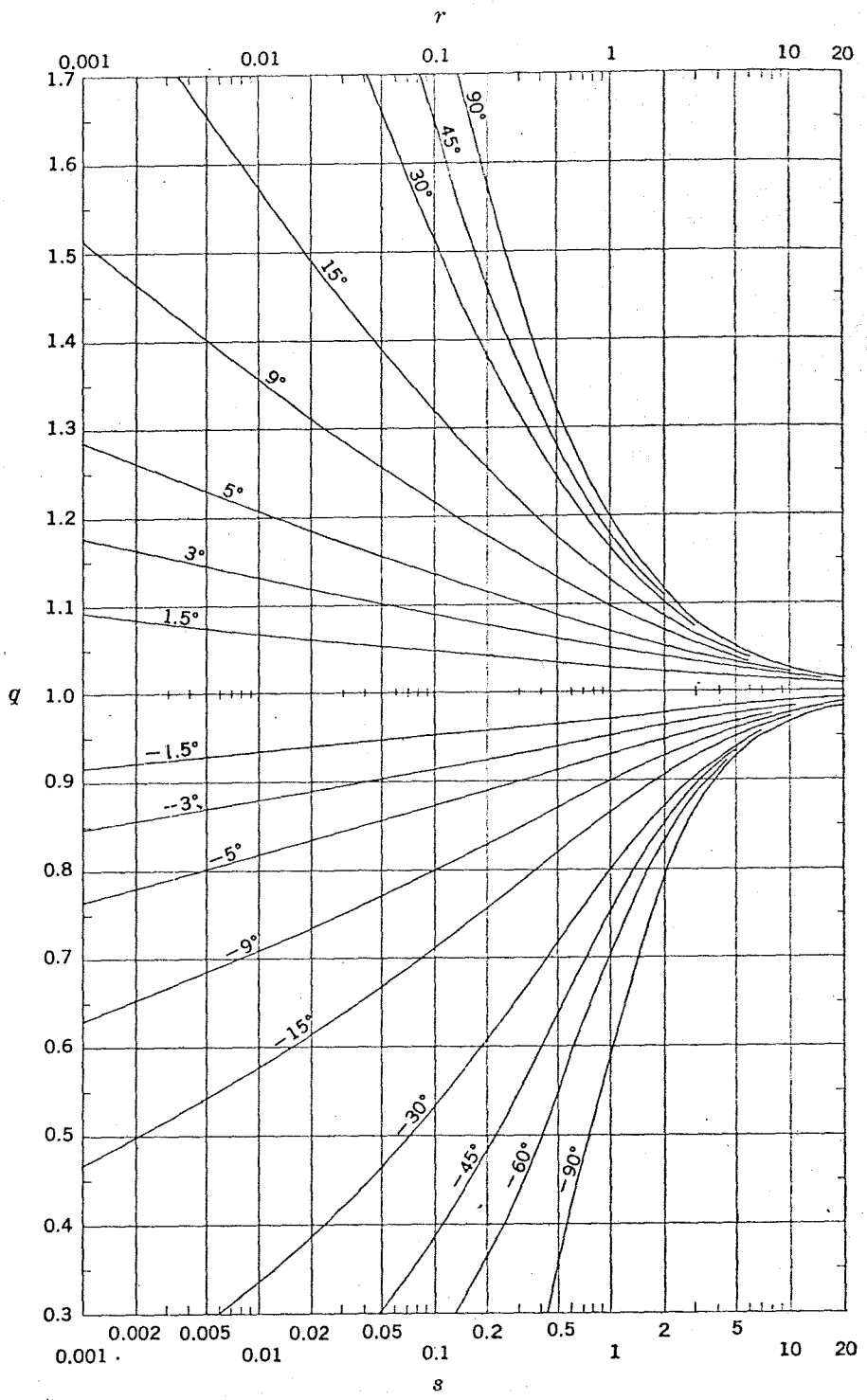

Fig. 3. Decay of the heat-flow anomaly with distance beyond the toe (r, upper curves) and behind the brink (s, lower curves) for selected slope angles (β).

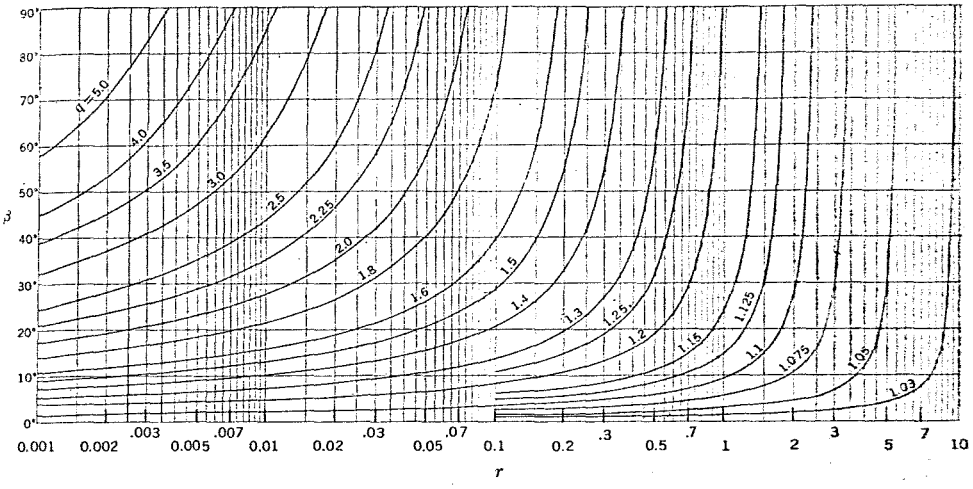

Fig. 4. Heat flow through the horizontal surface beyond the toe of a plane slope of angle β. r is distance from the toe in units of slope height.

s, r, and w will always be used as positive quantities and w will never exceed 1. Thus stations on the lower horizontal half plane will be designated by a value of the coordinate r, those on the upper half plane will be designated by a value of s, and those on the slope by a value of w. When a station lies on the lower half plane, i.e., beyond the toe, the relief will be referred to as 'positive,' and when it lies on the upper half plane (behind the brink), the relief will be

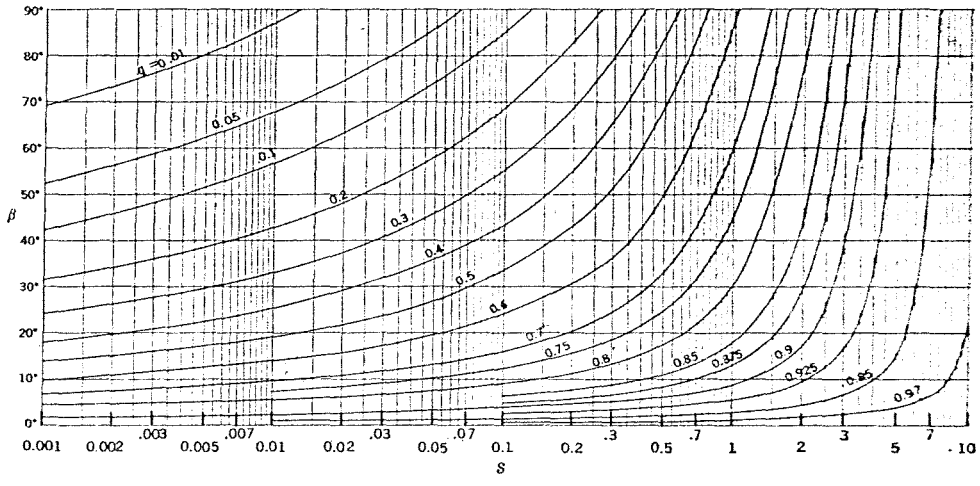

Fig. 5. Heat flow through the horizontal surface behind the brink of a plane slope of angle β. s is distance from the brink in units of slope height.

called 'negative.' Where it is not convenient to indicate the sign of the relief by explicit reference to the coordinates r and s, slopes below the station will be designated by a negative value of β and those above it by a positive value of β.

The general form of the normalized surface heat flow $q(x)$ is best seen from Figure 2, where the abscissa is in units of slope width. However, when dealing with effects beyond the toe or behind the brink, it is usually more convenient to consider distances in units of slope height. This is done in Figure 3, which shows the decay of the topographic anomaly as a function of r and s for selected slope angles. Although the analytical results are for $\beta = \pi/n$, n an integer, they are easily extended to other slope angles with graphs (Figures 4, 5, and 6). Tabular results are presented in Tables 1, 2, and 3. The quantity D in the tables represents the difference between the exact solution and the corresponding Jeffreys approximation (to be discussed in the next section).

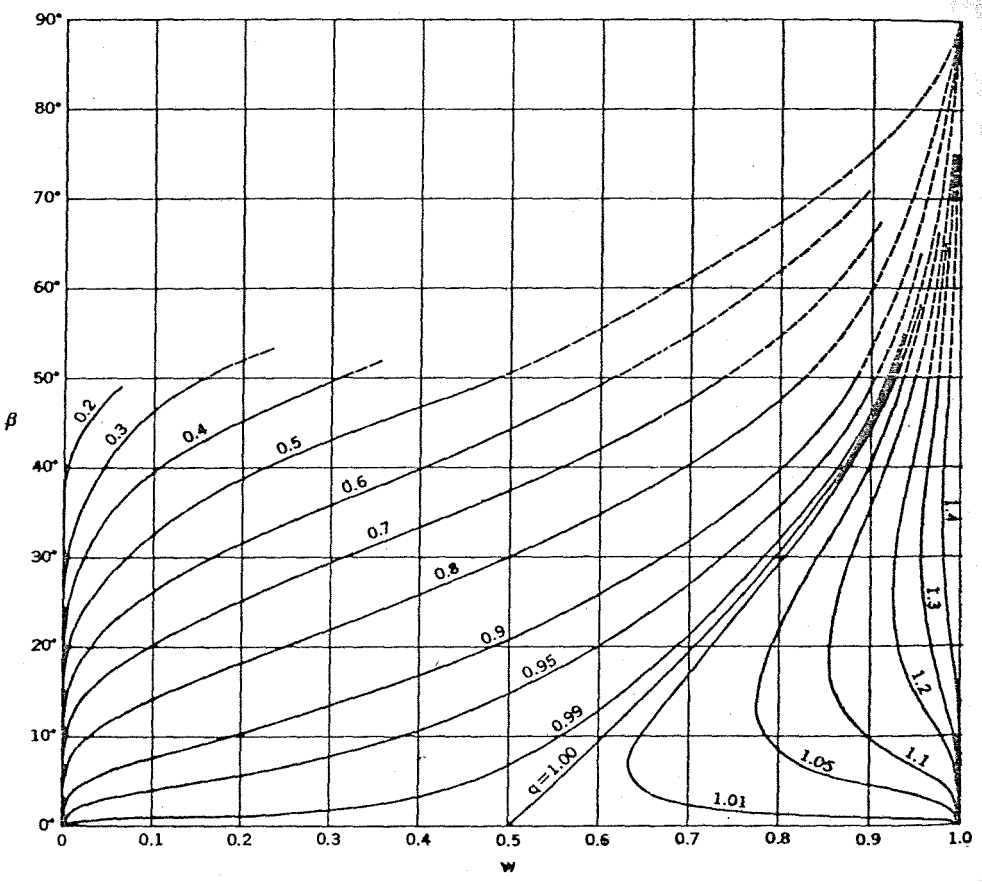

Fig. 6. Vertical component of heat flow through the sloping portion of a plane slope. w is horizontal distance from the brink in units of slope width.

ne slope. w the relief by tation will be ve value of β. est seen from when dealing convenient to which shows selected slope ger, they are l 6). Tabular tables repre- ding Jeffreys

TABLE 1. Normalized Heat Flow (q) on Horizontal Surface at Distance r beyond Toe of Plane Slope with Angle Beta and Unit Height (D is difference between exact solution and Jeffreys approximation)

B	90°		60°		45°		30°		15°		9°		5°		3°		1.5°	
r	q	D	q	D	q	D	q	D	q	D	q	D	q	D	q	D	q	D
20	1.015	- .0010	1.015	-.0009	1.015	-.0008	1.015	-.0007	1.014	-.0005	1.013	-.0003	1.012	-.0002	1.011	-.0001	1.009	-.0000
10	1.028	- .0034	1.028	-.0027	1.028	-.0024	1.027	-.0019	1.026	-.0012	1.024	-.0008	1.021	-.0004	1.018	-.0002	1.013	-.0000
7	1.039	- .0061	1.039	-.0048	1.038	-.0040	1.037	-.0031	1.035	-.0018	1.031	-.0011	1.026	-.0005	1.022	-.0002	1.016	-.0000
5	1.053	- .0107	1.052	-.0080	1.051	-.0066	1.050	-.0049	1.045	-.0026	1.040	-.0014	1.033	-.0006	1.026	-.0002	1.018	-.0000
3	1.082	- .0240	1.080	-.0166	1.079	-.0129	1.075	-.0088	1.065	-.0039	1.055	-.0018	1.043	-.0006	1.033	-.0002	1.022	+.0000
2	1.115	- .0445	1.111	-.0284	1.108	-.0210	1.101	-.0133	1.085	-.0051	1.070	-.0020	1.052	-.0005	1.039	-.0001	1.025	+.0000
1	1.196	- .1223	1.187	-.0640	1.178	-.0422	1.162	-.0227	1.126	-.0063	1.098	-.0018	1.070	-.0001	1.050	+.0001	1.031	+.0001
.7	1.254	- .2008	1.240	-.0918	1.226	-.0565	1.201	-.0276	1.151	-.0063	1.115	-.0014	1.080	+.0002	1.056	+.0003	1.034	+.0002
.5	1.321	- .3160	1.299	-.1242	1.279	-.0712	1.243	-.0316	1.176	-.0057	1.131	-.0006	1.089	+.0006	1.062	+.0005	1.037	+.0003
.3	1.448	- .6130	1.409	-.1827	1.374	-.0932	1.317	-.0349	1.218	-.0034	1.157	+.0011	1.104	+.0014	1.070	+.0009	1.041	+.0004
.2	1.575	- 1.017	1.515	-.2338	1.463	-.1078	1.383	-.0341	1.254	-.0002	1.179	+.0030	1.115	+.0022	1.078	+.0013	1.044	+.0005
.1	1.855	- 2.328	1.737	-.3173	1.644	-.1197	1.511	-.0233	1.319	+.0082	1.217	+.0073	1.136	+.0040	1.090	+.0020	1.050	+.0007
.07	2.035	- 3.512	1.874	-.3519	1.752	-.1165	1.585	-.0123	1.355	+.0140	1.238	+.0100	1.147	+.0050	1.096	+.0025	1.053	+.0009
.05	2.230	- 5.136	2.019	-.3759	1.863	-.1063	1.659	+.0018	1.389	+.0205	1.257	+.0130	1.158	+.0061	1.102	+.0029	1.056	+.0010
.03	2.580	- 9.030	2.268	-.3906	2.050	-.0754	1.779	+.0309	1.444	+.0322	1.288	+.0181	1.174	+.0080	1.111	+.0037	1.061	+.0012
.02	2.911	- 14.00	2.493	-.3793	2.216	-.0359	1.883	+.0608	1.490	+.0432	1.313	+.0227	1.186	+.0096	1.119	+.0043	1.064	+.0014
.01	3.602	- 29.23	2.943	-.3029	2.535	+.0659	2.076	+.1272	1.571	+.0654	1.357	+.0318	1.209	+.0127	1.132	+.0055	1.070	+.0017
.005	4.485	- 60.18	3.483	-.1397	2.905	+.2171	2.290	+.2144	1.656	+.0921	1.402	+.0424	1.232	+.0163	1.144	+.0069	1.077	+.0021
.001	7.568	-311.7	5.184	+.6772	3.999	+.8002	2.879	+.5086	1.875	+.1730	1.514	+.0729	1.286	+.0262	1.175	+.0107	1.091	+.0031

TABLE 2. Normalized Heat Flow (q) on Horizontal Surface at Distance s behind Brink of Plane Slope with Angle Beta and Unit Height
(D is difference between exact solution and Jeffreys approximation)

β	90°		60°		45°		30°		15°		9°		5°		3°		1.5°	
s	q	D	q	D	q	D	q	D	q	D	q	D	q	D	q	D	q	D
20	.9829	- .0011	.9834	- .0009	.9836	- .0008	.9840	-.0007	.9849	-.0005	.9858	-.0003	.9872	-.0002	.9887	-.0001	.9911	-.0000
10	.9642	- .0040	.9660	- .0031	.9671	- .0026	.9686	-.0020	.9717	-.0012	.9746	-.0008	.9784	-.0004	.9820	-.0002	.9868	-.0000
7	.9471	- .0074	.9509	- .0054	.9530	- .0044	.9561	-.0033	.9617	-.0018	.9666	-.0010	.9726	-.0005	.9779	-.0002	.9844	-.0000
5	.9231	- .0132	.9306	- .0091	.9348	- .0072	.9403	-.0050	.9499	-.0025	.9575	-.0013	.9664	-.0005	.9736	-.0002	.9820	-.0000
3	.8638	- .0300	.8845	- .0184	.8949	- .0135	.9076	-.0086	.9275	-.0035	.9413	-.0016	.9558	-.0005	.9666	-.0001	.9782	+.0000
2	.7878	- .0531	.8309	- .0293	.8508	- .0201	.8736	-.0118	.9061	-.0041	.9266	-.0016	.9466	-.0004	.9607	-.0000	.9750	+.0000
1	.5875	- .0942	.7027	- .0461	.7507	- .0286	.8010	-.0143	.8659	-.0035	.8989	-.0008	.9299	+.0001	.9502	+.0002	.9696	+.0001
.7	.4658	- .0795	.6245	- .0439	.6909	- .0266	.7589	-.0122	.8405	-.0021	.8839	+.0001	.9211	+.0005	.9447	+.0004	.9667	+.0002
.5	.3581	- .0053	.5493	- .0275	.6328	- .0175	.7180	-.0071	.8180	+.0001	.8695	+.0012	.9127	+.0010	.9395	+.0007	.9641	+.0003
.3	.2274	+ .2884	.4414	+ .0331	.5464	+ .0131	.6559	+.0074	.7835	+.0051	.8476	+.0035	.8999	+.0019	.9315	+.0011	.9600	+.0004
.2	.1546	+ .7461	.3662	+ .1146	.4825	+ .0528	.6082	+.0250	.7564	+.0105	.8302	+.0058	.8897	+.0028	.9252	+.0014	.9567	+.0005
.1	.0782	+ 2.261	.2623	+ .3170	.3866	+ .1499	.5323	+.0667	.7114	+.0223	.8010	+.0108	.8724	+.0046	.9145	+.0022	.9512	+.0007
.07	.0549	+ 3.602	.2201	+ .4465	.3441	+ .2121	.4964	+.0933	.6890	+.0297	.7862	+.0138	.8636	+.0057	.9090	+.0026	.9483	+.0009
.05	.0392	+ 5.405	.1863	+ .5809	.3080	+ .2771	.4645	+.1212	.6685	+.0374	.7725	+.0169	.8554	+.0068	.9038	+.0030	.9457	+.0010
.03	.0235	+ 9.634	.1445	+ .8029	.2601	+ .3857	.4197	+.1682	.6383	+.0504	.7521	+.0221	.8430	+.0086	.8961	+.0038	.9416	+.0012
.02	.0157	+ 14.93	.1181	+ .9908	.2274	+ .4789	.3872	+.2092	.6153	+.0617	.7363	+.0266	.8334	+.0102	.8899	+.0044	.9384	+.0014
.01	.0078	+ 30.84	.0835	+1.329	.1806	+ .6496	.3372	+.2855	.5778	+.0831	.7099	+.0351	.8170	+.0131	.8796	+.0056	.9330	+.0017
.005	.0039	+ 62.67	.0591	+1.682	.1433	+ .8314	.2936	+.3687	.5425	+.1069	.6845	+.0446	.8010	+.0164	.8693	+.0068	.9275	+.0021
.001	.0008	+317.3	.0264	+2.533	.0838	+1.283	.2127	+.5833	.4687	+.1702	.6289	+.0701	.7649	+.0252	.8459	+.0103	.9151	+.0030

Surface at Horizontal Distance w from Brink of Plane Slope with Angle Beta and Unit Width

.005	.0039	+ 62.67	.0591	+1.682	.1433	+ .8314	.2936	+.3687	.5425	+.1069	.6845	+.0446	.8010	+.0164	.8693	+.0068	.9275	+.0021
.001	.0008	+317.3	.0264	+2.533	.0838	+1.283	.2127	+.5833	.4687	+.1702	.6289	+.0701	.7649	+.0252	.8459	+.0103	.9151	+.0030

TABLE 3. Vertical Component of Heat Flow (q) on Sloping Surface at Horizontal Distance w from Brink of Plane Slope with Angle Beta and Unit Width (D is difference between exact solution and Jeffreys approximation)

β	45°		30°		15°		9°		5°		3°		1.5°	
w	q	D	q	D	q	D	q	D	q	D	q	D	q	D
.001	.0665	+.265	.2117	+.4810	.5120	+.1011	.6850	+.0332	.8172	+.0095	.8881	+.0033	.9432	+.0008
.005	.1138	+ .7987	.2922	+.2649	.5928	+.0442	.7456	+.0125	.8557	+.0031	.9127	+.0010	.9561	+.0002
.01	.1434	+ .6061	.3357	+.1802	.6315	+.0234	.7735	+.0051	.8729	+.0009	.9235	+.0002	.9617	+.0000
.03	.2072	+ .3136	.4189	+.0577	.6987	-.0048	.8202	-.0045	.9012	-.0020	.9412	-.0008	.9708	-.0002
.05	.2461	+ .1834	.4649	+.0060	.7329	-.0160	.8433	-.0082	.9149	-.0030	.9497	-.0012	.9751	-.0003
.07	.2760	+ .0994	.4984	-.0263	.7567	-.0227	.8592	-.0104	.9243	-.0036	.9555	-.0014	.9781	-.0004
.1	.3121	+ .0115	.5371	-.0591	.7834	-.0292	.8768	-.0125	.9346	-.0042	.9617	-.0016	.9813	-.0004
.2	.4001	- .1587	.6257	-.1195	.8414	-.0403	.9142	-.0159	.9562	-.0052	.9750	-.0019	.9880	-.0005
.3	.4682	- .2621	.6904	-.1539	.8817	-.0461	.9398	-.0175	.9708	-.0056	.9838	-.0020	.9924	-.0005
.4	.5299	- .3411	.7467	-.1788	.9156	-.0498	.9610	-.0185	.9829	-.0058	.9911	-.0021	.9961	-.0005
.5	.5908	- .4092	.8009	-.1991	.9474	-.0526	.9809	-.0191	.9941	-.0059	.9979	-.0021	.9995	-.0005
.6	.6560	- .4730	.8574	-.2171	.9800	-.0546	1.001	-.0195	1.005	-.0060	1.005	-.0021	1.003	-.0005
.7	.7319	- .5378	.9217	-.2340	1.016	-.0561	1.023	-.0197	1.018	-.0059	1.012	-.0021	1.007	-.0005
.8	.8316	- .6097	1.004	-.2505	1.062	-.0567	1.050	-.0194	1.033	-.0058	1.021	-.0020	1.011	-.0005
.9	.9982	- .7012	1.138	-.2660	1.132	-.0550	1.093	-.0180	1.056	-.0052	1.035	-.0018	1.018	-.0004
.93	1.086	- .7370	1.206	-.2689	1.168	-.0529	1.113	-.0169	1.067	-.0048	1.041	-.0016	1.021	-.0004
.95	1.173	- .7646	1.272	-.2687	1.201	-.0502	1.133	-.0156	1.078	-.0043	1.048	-.0014	1.024	-.0004
.97	1.311	- .7952	1.376	-.2628	1.252	-.0447	1.162	-.0132	1.093	-.0034	1.057	-.0011	1.029	-.0003
.99	1.651	- .8116	1.619	-.2254	1.365	-.0267	1.226	-.0057	1.127	-.0009	1.076	-.0002	1.038	-.0000
.995	1.903	- .7823	1.791	-.1823	1.441	-.0107	1.268	+.0007	1.148	+.0011	1.089	+.0005	1.044	+.0002
.999	2.633	- .5653	2.257	+.0127	1.631	+.0424	1.369	+.0206	1.200	+.0074	1.118	+.0028	1.058	+.0007

3. HEAT FLOW THROUGH A PLANE SLOPE: APPROXIMATE SOLUTION

It will be useful to obtain an approximate solution to the problem of the previous section. For this purpose we shall use the simplification of *Jeffreys* [1938], *Bullard* [1938], and *Birch* [1950], in which the irregular topographic surface is replaced by a plane reference surface whose temperature varies locally in proportion to the topographic relief.

To evaluate the topographic disturbance to temperature by this model at a point whose horizontal coordinate is x_0 and depth beneath the real surface is z, we pass the reference plane through $(x_0, 0)$ and assign to it the temperature

$$T(x) = Gh(x) \tag{2}$$

where G is the regional thermal gradient and $h(x)$ is the elevation of the topographic surface relative to the reference plane. (For simplicity, the topographic surface is considered isothermal in this part of the discussion.) Because the vertical gradient is treated as uniform in the topographic irregularities, the effects of heat which escapes horizontally through the sloping surfaces are neglected.

If the temperature disturbance is denoted by $\Delta\theta$, its gradient can be written

$$\frac{\partial \Delta\theta}{\partial z} = \frac{1}{\pi}\int_{-\infty}^{+\infty} T(x)\,\frac{(x-x_0)^2 - z^2}{[(x-x_0)^2 + z^2]^2}\,dx \tag{3}$$

At the surface, $z = 0$, the gradient disturbance approaches [Jeffreys, 1938; *TDT*, section 3]

$$\left.\frac{\partial \Delta\theta}{\partial z}\right|_{z=0} = \frac{1}{\pi}\int_{-\infty}^{+\infty} \frac{T(x)}{(x-x_0)^2}\,dx \tag{4}$$

If $Gg(x)$ and $Qq(x)$ represent the vertical gradient and heat flow at (x), then $g(x)$ and $q(x)$ represent these quantities normalized to the regional values G and Q. If we assume positive heat flow in the direction of decreasing z,

$$\frac{1}{G}\left.\frac{\partial \Delta\theta}{\partial z}\right|_{z=0} = g(x) - \frac{G}{G_0} = q(x) - \frac{Q}{Q_0} = \Delta q(x) = \Delta g(x) \tag{5}$$

G_0 and Q_0, denoting unit gradient and flux, are introduced for dimensional consistency. Throughout this paper 'heat-flow anomaly' will refer to the normalized (dimensionless) quantity, $\Delta q(x)$, which can be used interchangeably with $\Delta g(x)$, the normalized gradient anomaly. By 'heat flow' we shall always mean the normalized vertical heat flux

$$q(x) = 1 + \Delta q(x)$$

Equation 4 can be written

$$\Delta q(x_0) = \frac{1}{\pi G}\int_{-\infty}^{+\infty} \frac{T(x)}{(x-x_0)^2}\,dx \tag{6}$$

Note that equations 3, 4, and 6 can still be considered exact if T is considered as that function which properly represents the topographic relief at the reference plane.

Applying the Jeffreys assumption (equation 2) yields an approximation for

Δq which we denote by $\Delta q'$.

$$\Delta q'(x_0) = \frac{1}{\pi}\int_{-\infty}^{+\infty} \frac{h(x)}{(x - x_0)^2}\, dx \tag{7}$$

$\Delta q'$ and $q' = 1 + \Delta q'$ will be referred to as the 'Jeffreys approximation' to Δq and q, respectively.

For a plane slope of height H and angle β, (7) yields

$$q'(x) = 1 + \Delta q'(x) = 1 + \frac{1}{\pi}\tan\beta \ln\left(\frac{x}{x + H\cot\beta}\right) \qquad 0 < \beta < \frac{\pi}{2} \tag{8a}$$

$$= 1 - \frac{1}{\pi}\frac{H}{x} \qquad \beta = \frac{\pi}{2} \tag{8b}$$

Equations 8a and 8b apply for all x except the singular points $x = 0$ and $x = -H\cot\beta$. The quantity q and its approximation q' are compared for selected values of β in Figure 2, and their difference

$$D = q - q'$$

is illustrated in Figure 7 and tabulated in Tables 1, 2, and 3.

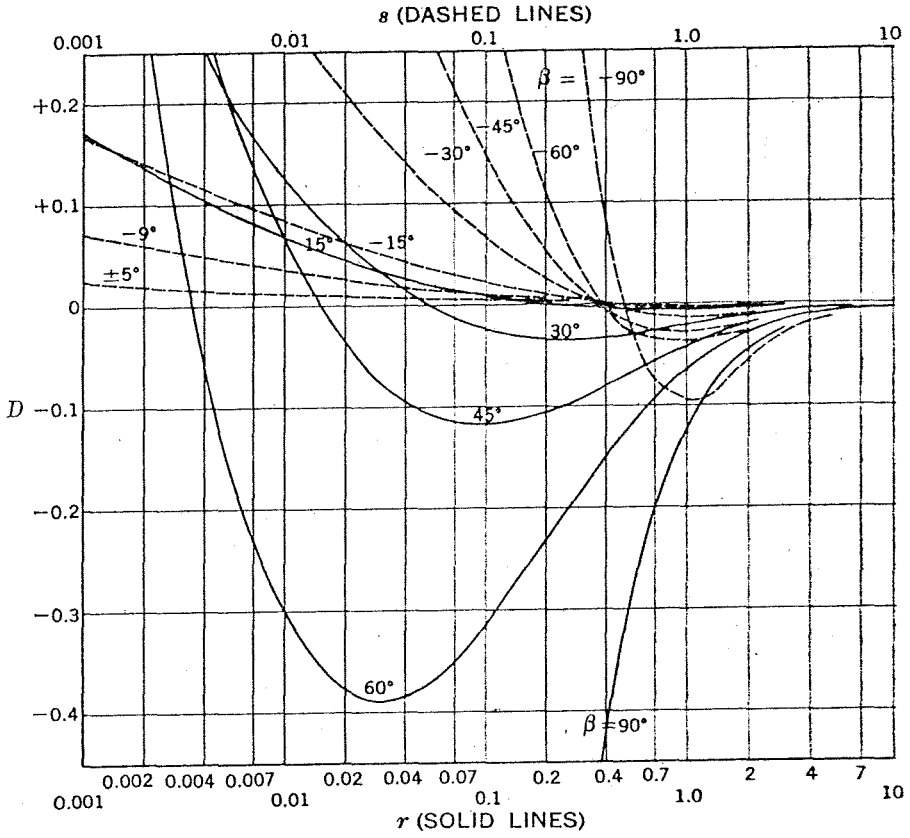

Fig. 7. Difference (D) between the exact solution and the Jeffreys approximation to the heat flow beyond the toe (solid lines) and behind the brink (dashed lines) of a plane slope for various angles (β).

Except for the case $\beta = +90°$, the Jeffreys approximation underestimates the heat flow near the toe and brink (positive D) and at greater distances overestimates it (negative D).

From equations 8 we see that $\Delta q'$ is symmetrical about the midpoint of the slope ($x = -0.5H \cot\beta$), and singularities occur at the brink and toe. The exact solution is asymmetrical; the negative infinite heat flow at the brink becomes zero heat flow in the exact solution, and heat flows are below the regional value over most of the slope. At the midpoint where $\Delta q'$ vanishes, the exact heat-flow anomaly Δq is given to a very good approximation by

$$\Delta q \approx -0.8 \sin^2 \beta \qquad x = -0.5H \cot \beta \tag{9}$$

It is clear from the figures and tables discussed that the difference D between q and q' generally decreases in magnitude with decreasing slope angle β and increasing distance from the slope.

This example shows the nature of the error in the Jeffreys approximation to surface heat flow near sharp topographic irregularities of a special kind. If a slight departure from the plane slope occurred near the measurement point, this error might look quite different. The Jeffreys approximation for the modified slope could be obtained, but an exact solution for it could not. Before the results for the plane slope can be useful, it is necessary to determine how to apply them to more general slopes, as there are no plane slopes on the earth's surface. This problem is considered in the sections that follow.

(If a general slope is approximated by a series of plane slopes and the exact contributions of each are added, it can be shown that the resulting approximation is not consistently better than the Jeffreys approximation.)

4. HEAT FLUX ON A HORIZONTAL SURFACE BETWEEN TWO PLANE SLOPES

It has been pointed out that the plane slope is a highly idealized topographic form but that more complicated exact models generally lose the advantage of the two-parameter representation or of intuitive simplicity. To extend the results to characterize more general configuration is worthwhile, and it can be done with limited success for the heat flux on a horizontal surface between two plane slopes. There are three cases. In the first (Figure 8*a*), the station lies on the horizontal surface between two positive plane slopes, $h_a(x)$ and $h_b(x)$. We shall call this the 'plane valley.' In the second case, the 'plane ridge' (Figure 8*b*), the station lies on the horizontal surface between two negative plane slopes. The third case is the 'plane bench' (Figure 8*c*) in which the station lies on the horizontal surface between plane slopes of opposite sign.

The surface heat flux will be considered at a point x_0 on the horizontal surface—strip $a > x > b$ (Figure 8). The heat flow $q(x_0)$ cannot be obtained by simply adding the heat-flow anomalies, $\Delta q_a(x_0)$ and $\Delta q_b(x_0)$, of the independent plane slopes because the presence of h_a modifies the heat flow through h_b (and conversely) and the modification, in turn, further modifies the heat flow through h_a and so on. There is, however, a hypothetical temperature distribution

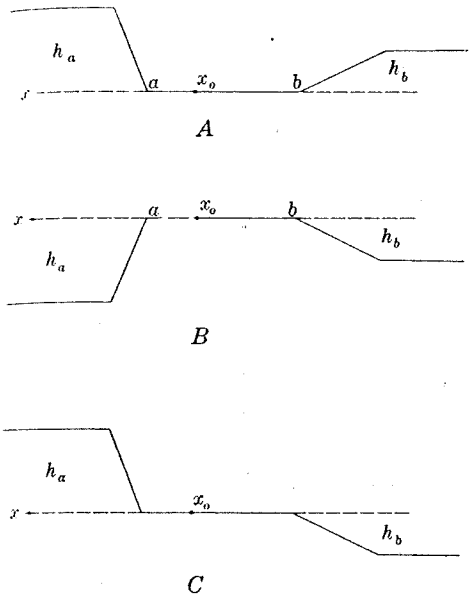

Fig. 8. Coexisting plane slopes forming (*A*) a plane valley, (*B*) a plane ridge, and (*C*) a plane bench.

$T(x)$ over the plane $z = 0$ that will affect the heat flow at x_0 in the same way as the isothermal topographic surface $h(x) = h_a(x) + h_b(x)$. Although the plane slopes are not superimposable in the geometric sense, the collective contributions to the reference-plane temperature are. By considering upper and lower limits to these contributions, we obtain the following inequalities (*TDT*, section 5).

Case 1. The plane valley; $h_a(x), h_b(x) > 0$.

$$\Delta q(x_0) > \Delta q_a(x_0) + \Delta q_b(x_0) \tag{10a}$$

$$\Delta q(x_0) < \Delta q_a(x_0)[1 + \Delta q_b(a) + \Delta q_a(b)\,\Delta q_b(a) + \Delta q_b(a)\,\Delta q_a(b)\,\Delta q_b(a) + \cdots] + \Delta q_b(x_0)[1 + \Delta q_a(b) + \Delta q_b(a)\,\Delta q_a(b) + \Delta q_a(b)\,\Delta q_b(a)\,\Delta q_a(b) + \cdots] \tag{10b}$$

Case 2. The plane ridge; $h_a(x), h_b(x) < 0$.

$$\Delta q(x_0) > \Delta q_a(x_0) + \Delta q_b(x_0) \tag{11a}$$

$$\Delta q(x_0) < \Delta q_a(x_0)[1 + \Delta q_b(a)] + \Delta q_b(x_0)[1 + \Delta q_a(b)] \tag{11b}$$

Case 3. The plane bench; $h_a(x) > 0, h_b(x) < 0$.

$$\Delta q(x_0) > \Delta q_a(x_0)[1 + \Delta q_b(a) + \Delta q_a(b)\Delta q_b(a)] + \Delta q_b(x_0)[1 + \Delta q_a(b)] \tag{12a}$$

$$\Delta q(x_0) < \Delta q_a(x_0) + \Delta q_b(x_0)[1 + \Delta q_b(a)\Delta q_a(b) + (\Delta q_a(b))^2 \Delta q_b(a)] \tag{12b}$$

As an example of the application of these relations, consider the anomaly $\Delta q(x_0)$ at the midpoint of a bench of width $2H$ bounded by 45° slopes of height H. From Tables 1 and 2

$$\Delta q_a(x_0) = \Delta q(45°, r = 1) = +0.178$$

$$\Delta q_a(b) = \Delta q(45°, r = 2) = +0.108$$

$$\Delta q_b(x_0) = \Delta q(45°, s = 1) = -0.249$$
$$\Delta q_b(a) = \Delta q(45°, s = 2) = -0.149$$

By (12)

$$\Delta q(x_0) > -0.127$$
$$\Delta q(x_0) < -0.067$$

hence

$$0.87 < q(x_0) < 0.93$$

By comparison the Jeffreys approximation gives

$$q'(x_0) = 1.00$$

As a second example, consider a ridge of width $2H$ bounded by 45° slopes of height H. The heat flow at a point x_0, $0.1H$ from point a and $1.9H$ from point b, is found from (11) and Table 2 to be

$$0.23 < q(x_0) < 0.34$$

For the same case the Jeffreys approximation yields

$$q'(x_0) = 0.10$$

In summary, a lower limit to the heat-flow anomaly on the horizontal surface between two plane slopes (h_a and h_b) of the same sign (cases 1 and 2) is provided by the sum of the independent exact solutions for each slope [$\Delta q_a(x_0) + \Delta q_b(x_0)$]. The upper limit is provided by adding an overestimate of interaction effects. If the horizontal surface lies between plane slopes of opposite sign (case 3), both the upper and lower limits contain interaction terms, but the sum of the independent exact solutions forms the upper limit to terms of second order in the interaction. In all three cases the bracketing interval ($q_{\text{upper}} - q_{\text{lower}}$) is represented by the first-order interaction terms with or without higher-order effects.

$$q_{\text{upper}} - q_{\text{lower}} = |\Delta q_a(x_0)\Delta q_b(a) + \Delta q_b(x_0)\Delta q_a(b)| + \text{higher order} \qquad (13)$$

But

$$|\Delta q_a(x_0)| > |\Delta q_a(b)|$$
$$|\Delta q_b(x_0)| > |\Delta q_b(a)|$$

Hence

$$\Delta q(x_0) \approx \Delta q_a(x_0) + \Delta q_b(x_0) + [\Delta q_a(x_0)\ \Delta q_b(x_0)][1 \pm 1] \qquad (14)$$

in all three cases if higher-order terms are neglected. These results are not restricted to plane slopes; they apply to any topographic elements h_a and h_b for which $|\Delta q_a|$ and $|\Delta q_b|$ decrease with distance from the toe and brink.

In all these cases the Jeffreys approximation gives surprisingly good results over a wide variety of conditions. It can, however, contain considerable error at points very near steep slopes.

5. GEOMETRIC BRACKETING

Useful upper or lower limits to the superficial effects of fairly general features can sometimes be determined quickly from the results for plane slopes selected to overestimate or underestimate the effects.

Let $h(x)$ be a general two-dimensional surface and $h_u(x)$ and $h_l(x)$ be two other surfaces such that

$$h_u(x) \geq h(x) \geq h_l(x) \qquad +\infty > x > -\infty \tag{15}$$

The heat-flow anomalies on each surface are denoted respectively by $\Delta q_u(x)$, $\Delta q(x)$, and $\Delta q_l(x)$. It can be shown (*TDT*, section 6) that at any point x_0 (not a sharp corner) at which

$$h_u(x_0) = h(x_0) \tag{16a}$$

we have

$$\Delta q_u(x_0) > \Delta q(x_0) \tag{16b}$$

and where

$$h(x_0) = h_l(x_0) \tag{17a}$$

then

$$\Delta q(x_0) > \Delta q_l(x_0) \tag{17b}$$

It follows that where

$$h_u(x_0) = h(x_0) = h_l(x_0) \tag{18a}$$

we have

$$\Delta q_u(x_0) > \Delta q(x_0) > \Delta q_l(x_0) \tag{18b}$$

Equations 15 to 18 will be referred to as the theorem on geometric bracketing. It is illustrated in Figure 9, where $h(x)$ is represented by the horizontal lines OL and $U'P$ and the wavy line Lt_1t_2U' joining them. The plane slope $OUU'P$ represents h_u and the plane slope $OLL'P$ represents h_l. Then (18) applies for all points (x_0) on OL and $U'P$. One-sided limits are given at the points of tangency, $x_0 = t_1$ (relations 16) and $x_0 = t_2$ (relations 17).

The results of this section can be applied to those of section 4 to establish limits to the heat-flow anomaly at stations interior to many real valleys, ridges, and benches or to section 2 to obtain limiting values to the anomaly near simpler slopes.

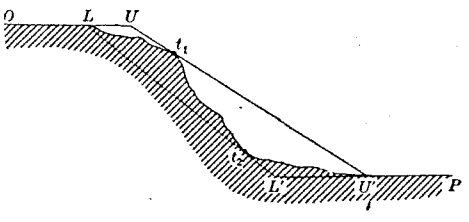

Fig. 9. Geometric bracketing of a general slope with two plane slopes.

The method of geometric bracketing can quickly lead to a determination of whether specific topographic features are significant in heat-flow studies. For example, the effect of any positive feature is overestimated by that of a cliff of the same height and distance from the station. Thus a positive feature whose height is less than 10% of its distance from the station cannot affect the heat flow there by more than 2.8% (Table 1); if its height is 5% of the distance, the limit is 1.5%. The corresponding limits for negative features are 3.6% and 1.7%. (It is surprising that the anomaly 10 slope heights from the toe of a 90° cliff, 2.8%, is not very different from the anomaly 10 slope heights from the toe of a 5° slope, 2.1%, Table 1.) If features of the same sign occur at such distances on both sides of the station, their interaction would be negligible (relation 14), and the limiting effects are obtained by adding the individual limits. If the features are of opposite sign, the limiting effect is the one having the larger magnitude. Other examples can quickly be taken from Table 1. A positive slope whose height is equal to its distance from the station cannot affect the heat flow by more than 10% if its maximum slope angle is 9°. A valley 1 km deep with a 10-km flood plane will not increase the heat flow at its center by more than 10% if the walls are not steeper than 30°. (The interaction is negligible by (14).)

If holes are drilled to determine heat flow, it is desirable to select sites at which the topographic anomaly is minimized. Thus site selection often involves making many calculations of the type just discussed. I have found it helpful to take a copy of Figure 3 to the field for this purpose.

Although the bracketing described is achieved with a two-dimensional model, it can, of course, be applied to three-dimensional topographic forms.

6. EQUIVALENT SLOPES

The methods of the preceding section often give a useful upper or lower limit to the topographic anomaly, but the condition that the bracketing slopes be present everywhere above or below the real surface usually leads to bracketing intervals that are rather large. A more refined method is therefore considered in this section.

Returning to the discussion of section 3, we see that an exact expression analogous to the approximation (7) can be obtained from (6) if the Jeffreys assumption (2) is replaced by

$$T(x) = Gh(x)[1 + e(x)]$$

where e is the unknown function that adjusts (2) to give the required value of T at the reference plane.

$$\Delta q(x_0) = \frac{1}{\pi}\int_{-\infty}^{+\infty} \frac{h(x)[1+e]}{(x-x_0)^2}\,dx \tag{19}$$

$$= \Delta q'(x_0) + \frac{1}{\pi}\int_{-\infty}^{+\infty} \frac{h(x)e}{(x-x_0)^2}\,dx \tag{20}$$

$$D(x_0) = \Delta q(x_0) - \Delta q'(x_0) = \frac{1}{\pi}\int_{-\infty}^{+\infty} \frac{h(x)e}{(x-x_0)^2}\,dx \tag{21}$$

It is seen that $e(x)$ can be viewed (for positive $h(x)$) as the mean value of the gradient disturbance at (x) between the topographic surface and the reference plane, or the mean value of the heat-flow disturbance there. (For negative h, it is, of course, a fictitious quantity but no less useful as a concept.) Thus e is positive where the topography concentrates the vertical flux, generally near the toe of a slope. It is negative where the vertical flux is attenuated by the relief, generally near the brink of a slope. (Its value must be greater than -1 over any finite interval if overhanging topography is excluded.) Thus a bump on a plane slope generally contributes more to the reference plane temperature if it occurs near the toe (positive e) than near the brink (negative e). This notion forms the basis for the approximating schemes of this section.

To discuss rather general topographic features and still restrict consideration to slope-like forms, we shall define a 'slope form' as two horizontal half planes joined by a general (two-dimensional) surface whose highest point is the intersection with upper half plane (the brink) and whose lowest point is the intersection with the lower half plane (the toe). If no ambiguity will result, this figure will be referred to simply as a 'slope.'

Consider a slope form $h_{ab}(x)$ as the sum of a plane slope $h_a(x)$ and the irregular surface of finite width, h_b. The anomaly at a point x_0 on the horizontal portion is (19, 20)

$$\Delta q_{ab}(x_0) = \frac{1}{\pi}\int_{-\infty}^{+\infty} \frac{h_{ab}(1+e_{ab})}{(x-x_0)^2}\,dx$$
$$= \Delta q_a(x_0) + \Delta q_b'(x_0) + \frac{1}{\pi}\int_{-\infty}^{+\infty} \frac{h_b e_a}{(x-x_0)^2}\,dx + \frac{1}{\pi}\int_{-\infty}^{+\infty} \frac{h_{ab}(e_{ab}-e_a)}{(x-x_0)^2}\,dx \tag{22}$$

In this way the anomaly due to a rather general surface can be expressed in terms of the anomaly due to a plane slope plus correction terms.

If we choose a plane slope h_a which yields the same Jeffreys approximation at x_0 as the given slope h_{ab}, then

$$\frac{1}{\pi}\int_{-\infty}^{+\infty} \frac{h_{ab}-h_a}{(x-x_0)^2} \equiv \Delta q_b' = 0$$

and the second term of (22) vanishes. The choice also ensures canceling effects in the third and fourth terms. Such slopes, yielding the same Jeffreys approximation at a point x_0, will be referred to as '*equivalent at* x_0.' It is clear that any two slopes equivalent to a third slope at x_0 are equivalent to each other there. For any slope h_{ab} there is a family of plane slopes equivalent to it at any point x_0 not on the slopes. This can be seen by noting that, given $\hat{h}_a$ equivalent to h_{ab} (Figure 10), another slope, $h_a{}^*$, equivalent to $\hat{h}_a$ can be drawn by increasing the slope angle and distance from the station simultaneously in such a way as to keep $\Delta q_a'$ constant. Thus, the flatter the equivalent plane slope, the closer it extends toward the station. The 'equivalent cliff' is the member of the family farthest from the station. In general it is found that flatter members of the family yield algebraically larger anomalies, Δq_a, irrespective of the sign of the slope. Thus for any slope h_{ab} it is possible to bracket the exact effect at x_0 by finding flatter and steeper plane slopes equivalent there (*TDT*, section 7).

For example, the plane slope $\hat{h}_a$ is flatter than the slope h_{ab} (Figure 10) in the sense that they cross at only one point, so that $\hat{h}_b$ is composed of one negative region ($\hat{h}_{b_1}$) near the toe and one positive region ($\hat{h}_{b_2}$) near the brink. Because $\hat{e}_a$ is greater near the toe, the third term in (22) takes the sign of $\hat{h}_{b_1}$. The third term generally dominates the fourth (*TDT*, section 6), and hence

$$\Delta q_{ab}(x_0) < \Delta \hat{q}_a(x_0)$$

Similarly the steeper equivalent slope h_a^* yields a lower limit to Δq_{ab} because it makes the third term in (22) positive. Generally

$$\Delta q^*(x_0) < \Delta q(x_0) < \Delta \hat{q}(x_0) \tag{23}$$

where the asterisk denotes quantities associated with a steeper equivalent plane slope and the circumflex denotes a flatter one. If the given feature is a slope form, such bracketing plane slopes can always be found for points, x_0, beyond the toe or behind the brink. The inequality (23) can be violated for very special shapes, h_{ab}, that are generally unimportant in physical applications. Also, for points very close to the brink where the heat flow is close to zero, higher-order effects can invalidate (23). These departures are small, and they can generally be checked by geometric bracketing (see example, this section).

Bracketing with equivalent plane slopes can usually be accomplished quickly with the following steps:

(1) Determine $\Delta q'$ for the given slope. This can often be done by breaking it into component plane slopes and adding the contributions determined from Figure 11.

(2) Select a steeper equivalent plane slope (h^*) and a flatter one ($\hat{h}$) from the family represented by the appropriate ordinate line, $\Delta q'$, Figure 11. (The smallest bracketing interval is achieved by selecting the permissible $\hat{h}$ farthest from the station and h^* closest to it.

(3) Determine $\Delta \hat{q}$ and Δq^* from Figure 4 or 5.

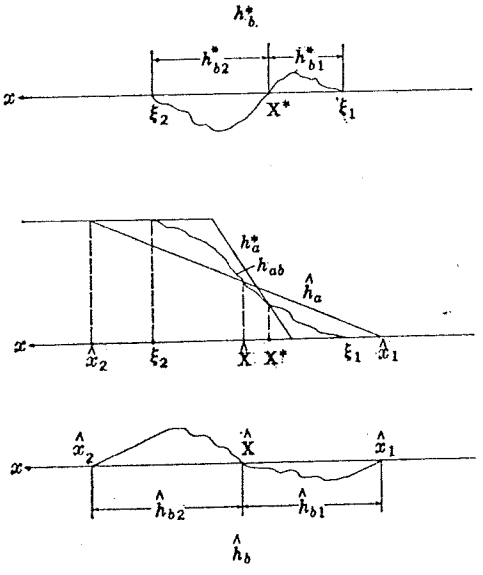

Fig. 10. Notation for the discussion of equivalent plane slopes (h_a^* and $\hat{h}_a$).

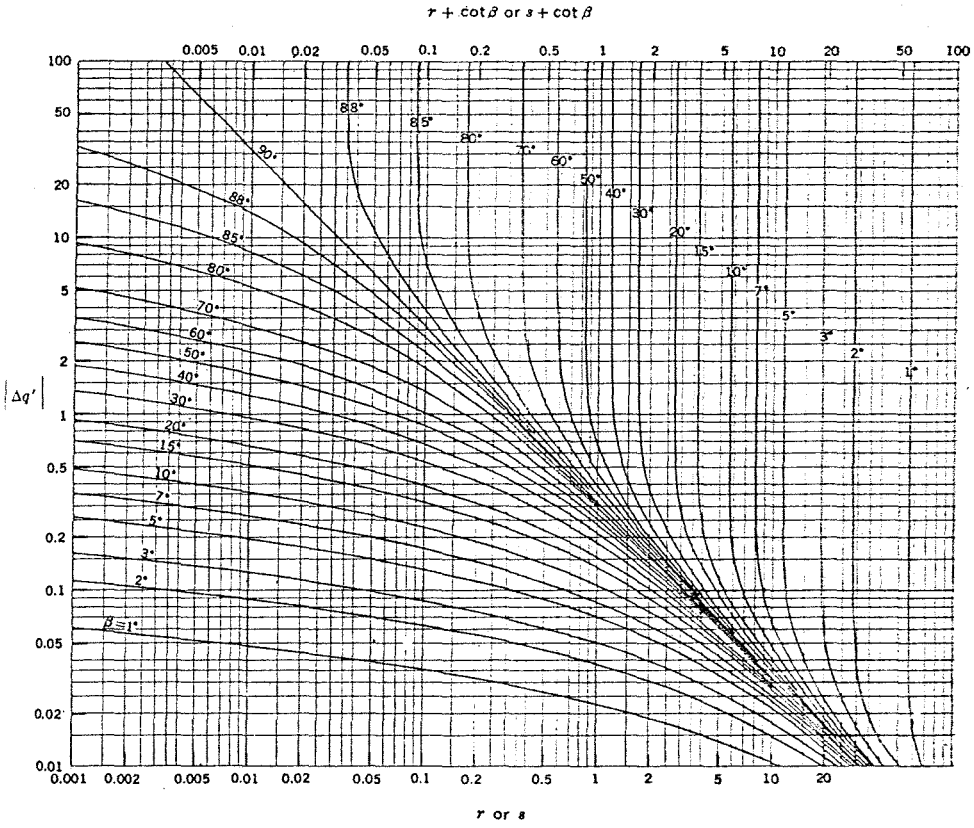

Fig. 11. Jeffreys approximation ($\Delta q'$) as a function of distance from the toe or brink of a plane slope, whichever is closest to the station (r or s, and lower left curves), or whichever is farthest from the station ($r + \cot\beta$ or $s + \cot\beta$, and upper right curves).

Because the slopes represented by the three parts of (23) are equivalent, each is associated with the same Jeffreys approximation, $\Delta q'$. Subtracting this from (23) yields

$$D^*(\beta^*, \Delta q') < D < \hat{D}(\hat{\beta}, \Delta q') \tag{24}$$

The discrepancy (D) in the Jeffreys approximation is shown as a function of the Jeffreys approximation ($\Delta q'$) for plane slopes of various slope angles (solid lines) or distances from the station (dashed lines) in Figures 12 and 13. This representation provides additional insight and short cuts for estimating anomalies. Vertical coordinate lines represent families of equivalent slopes $\Delta q'(\beta, r)$ = constant (Figure 12) or $\Delta q'(\beta, s)$ = constant (Figure 13). The members of the family can be identified by the curves of constant β and r (or s). Given any positive slope for which $\Delta q' = 0.6$, and which can be bracketed (in the sense of Figure 10) by plane slopes with $\hat{\beta} = 45°$ and $\beta^* = 60°$, it is seen from Figure 12 that D lies between -0.11 and -0.18 and hence $1.42 < q < 1.49$.

Most natural slopes decrease in inclination near the toe and brink, making it

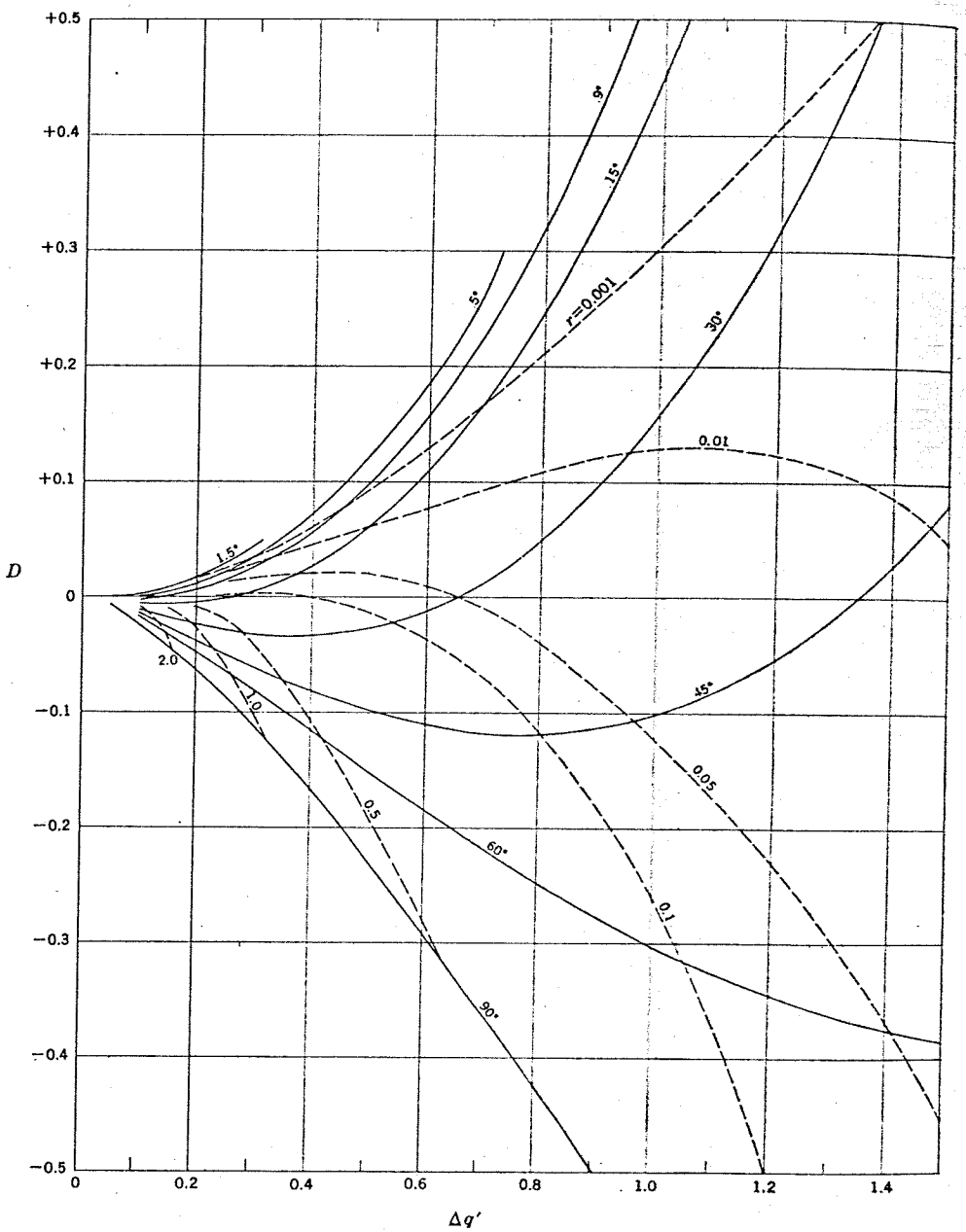

Fig. 12. Error in the Jeffreys approximation (D) as a function of the Jeffreys approximation ($\Delta q'$) for constant positive slope angle, β (solid curves), or constant distance from the toe, r (dashed curves).

possible to draw $\hat{h}$ through the toe for positive slopes and through the brink for negative slopes. (Such slopes are referred to as 'concave at the toe' or 'convex at the brink,' *TDT*, section 6.) The station is the same distance (r or s) from such slopes as it is from $\hat{h}$. Thus, from Figure 12, any positive slope, concave at the toe,

whose height does not exceed 20 times its distance to the station ($r = 0.05$) and whose maximum inclination does not exceed 30°, can be represented by the Jeffreys approximation with errors not exceeding 3%. (Such slopes can be bracketed by equivalent plane slopes which lie in the region between curves $r = 0.05$ and $\beta = 30°$.) Other conditions for validity or failure of the Jeffreys approximation can readily be obtained from Figures 12 and 13. From Figure 13 it is seen that negative slopes, convex at the brink, can be approximated by the Jeffreys method to within 3% if their height does not exceed about 3 times their distance from the station and the maximum slope angle does not exceed about 45°. Almost any slope, positive

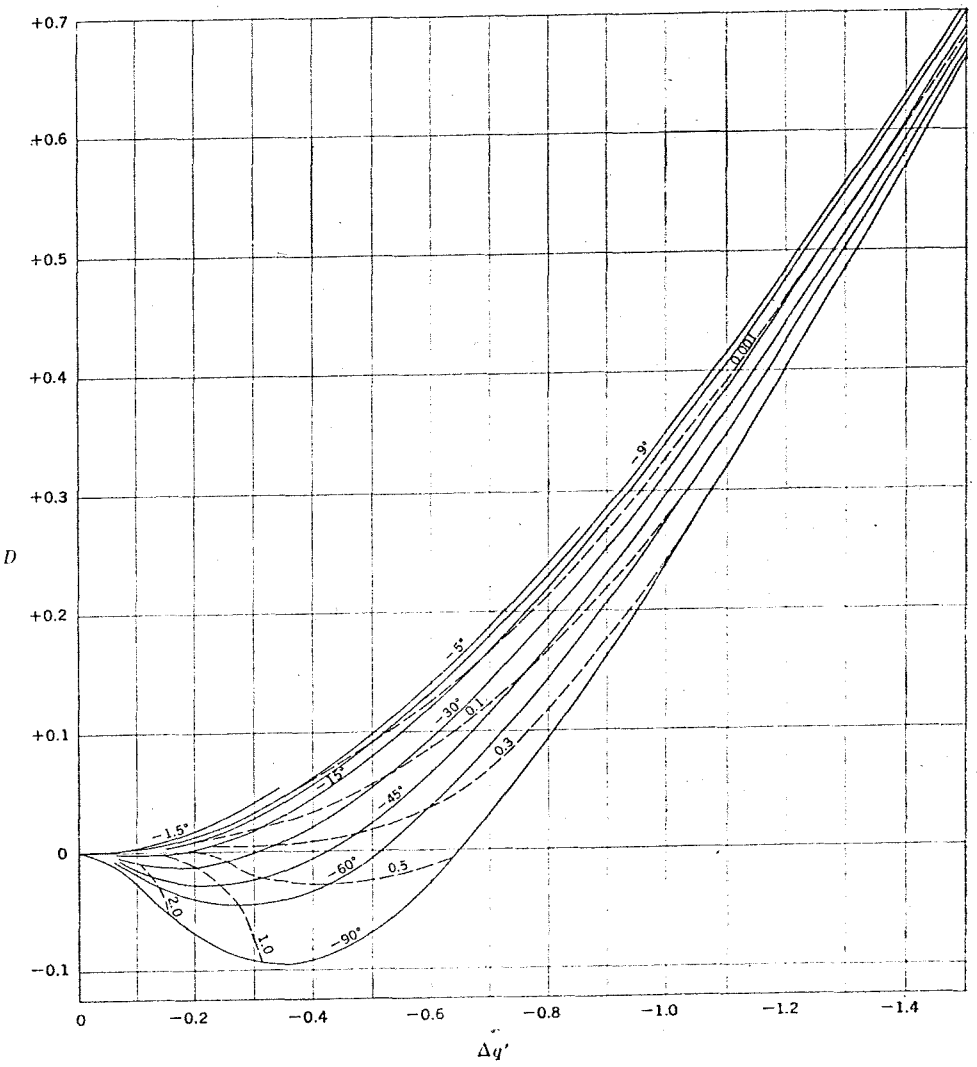

Fig. 13. Error in the Jeffreys approximation (D) as a function of the Jeffreys approximation ($\Delta q'$) for constant negative slope angle, β (solid curves), or constant distance from the brink, s (dashed curves).

or negative, irrespective of slope at the toe or brink, can be represented by the Jeffreys approximation within a few per cent as long as $\Delta q'$ does not exceed 0.15 and $\beta^* < 60°$.

In general it is seen (Figure 13) that for negative slopes the Jeffreys approximation is poor when $\Delta q'$ is large because the approximation becomes negatively infinite at the brink where the actual heat flow approaches zero.

Three points should be emphasized: (1) Although the Jeffreys approximation might apply to the independent effects of slopes on either side of a station, it does not apply in general when the two co-exist. Their interaction must be considered, as it must for any other slopes. (2) Small $\Delta q'$ is not a sufficient condition for validity of the Jeffreys approximation unless co-existing slopes are of the same sign. (3) Effects of a given monocline-like slope can be represented well at a station by selecting an equivalent slope to approximate (not bracket) there. (See example of next section.) Conversely, if plane slopes are used for calculation of effects of hypothetical topography (as in the case of unseen relief on the ocean bottom, section 8), they can be viewed as representing a variety of much more general equivalent forms.

As a numerical example of bracketing with equivalent plane slopes, consider the anomaly one-tenth of a hill height behind the slope illustrated in Figure 14.

Step 1. From Table 2 or Figure 11

$$\Delta q_{ab}'(s = 0.1) = \Delta q'(90°, s = 0.2) + \Delta q'(45°, s = 0.2) = -2.16$$

Step 2. To obtain the smallest bracketing interval, h^* is picked through the brink and $\hat{h}$ through the toe with the aid of Figure 11.

$$\beta^* = 84°, \qquad s^* = 0.1$$

$$\hat{\beta} = 60°, \qquad \hat{s} = 0.600 - \cot 60° = 0.023$$

Step 3. Figure 5 and (23) yield

$$0.11 < q_{ab}(s = 0.1) < 0.13 \tag{25}$$

By contrast, the Jeffreys approximation yielded (step 1)

$$q_{ab}' = -1.16$$

and the sum of exact solutions for slope components (Figure 5 or Table 2)

$$q_{ab} \approx 1 + \Delta q(90°, s = 0.2) + \Delta q(45°, s = 0.2) = -0.36$$

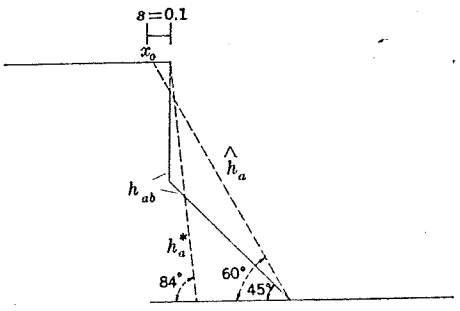

Fig. 14. Illustration of numerical example, section 6.

The second two results are, of course, physically impossible, as q_{ab} cannot be a negative quantity.

In this example x_0 was very close to the brink, where, as we have seen, the left side of the inequality (23) might not be rigorously correct. If we had chosen $\beta^* = 90°$ instead of 84°, the same lower limit (to two significant figures in equation 25) would have resulted. If, however, there is concern about the lower limit given by (23) in cases like this, we can resort to simple geometric bracketing which yields

$$q(90°, s = 0.1) < q_{ab}(s = 0.1)$$

and, from Figure 5 or Table 2,

$$0.08 < q_{ab}(s = 0.1)$$

This demonstrates that the lower limit of 0.11 in (25) cannot be much in error.

7. STATIONS ON GENTLY SLOPING SURFACES

Many of the results of the preceding sections apply only to stations lying on geometrically horizontal surfaces, although these stations may be very close to steep and irregular slopes. The earth's surface cannot be considered geometrically horizontal over extended areas, but much of it is inclined at angles of less than a degree or two. Although slope angles may change very rapidly near the toe and brink of topographic scarps, the distant transition to horizontalness is generally gradual. Many heat-flow stations requiring topographic correction will lie on gently sloping surfaces adjacent to bold features. It is necessary to consider how to apply the foregoing results to stations on such surfaces.

It can be shown (*TDT*, section 8) that if the topography is gently sloping in the vicinity of a station ($x = 0$) and smooth in the sense that the surface and the heat flow through it can be represented by a few terms of Maclaurin's series, then the topographic anomaly can be computed by flattening the slope in the vicinity of the station, as illustrated in Figure 15. The true slope h_{ab} is replaced by the slope h_a, which is flattened over the interval $|x| < l/2$ and adjusted upward or downward to eliminate discontinuities $x = \pm l/2$.

If $\gamma(x)$ denotes the slope of the tangent to $h_{ab}(x)$ measured clockwise from negative x and

$$\Delta\gamma = \gamma(l/2) - \gamma(-l/2)$$

$$\Lambda = \frac{q_{ab}(l/2) - q_{ab}(-l/2)}{q_{ab}(0)}$$

then the error due to flattening can be expressed as

$$\frac{q_{ab}(0) - q_a(0)}{q_{ab}(0)} \approx \frac{1}{\pi} [\tan \Delta\gamma + 2\Lambda \tan \gamma(0)] \qquad (26)$$

The result accounts for the reaction of close-in topography to higher-order effects of distant topography but neglects the much smaller higher-order effects of

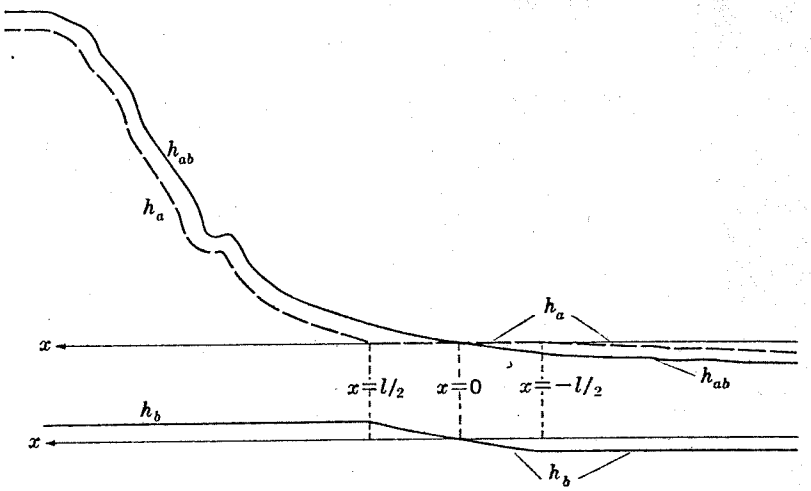

Fig. 15. The general slope, h_{ab}, represented as the sum of the flattened slope h_a and the increment h_b.

close-in topography acting through distant topography. It is seen that the absolute error $|q_{ab}(0) - q_a(0)|$ is independent of the heat flow if the curvature is negligible and independent of the slope if the lateral change of heat flow is negligible.

If the change in slope ($\Delta\gamma$) over the flattened interval is less than 2°, the curvature term will not contribute more than 1% to the error; if it is less than 5°, the contribution will be less than about 2½%. In general, Λ, the relative change in heat flow across the flattened interval, will not be known, but inspection of the slope will normally permit an estimate of its order of magnitude. If Λ is 50%, a rather extreme case, the second term will contribute about 1% to the error if the slope at the station is 2°. If Λ is 20%, a 5° slope will contribute 1%.

Equation 26 probably should not be used for $\Delta\gamma$ and γ_0 much larger than 5° or 6° because of the condition, $2|h_b\ (\pm l/2)\ |l^{-1} \ll 1$, required in the approximation. When Λ is large, $q_{ab}(x)$ is likely to have considerable curvature in $|x| < l/2$; and this can be tolerated in (26) if $\Delta\gamma$ is very small. If not, it is probably best to restrict the application to cases in which Λ does not exceed 25% or so. This will include most cases of interest.

It is seen that, after the flattening procedure is applied, most stations will lie on the horizontal surface between two co-existing slopes (the valley, ridge, or bench, section 5), one of which can often be neglected.

As a combined example of the flattening procedure, approximating with equivalent slopes, and the results of section 4, we consider the surface heat flow in the vicinity of the brink ($x_0 = +0.55$) of a 'monocline' of the type considered by *Jaeger and Sass* [1963, equation 11 with $\alpha = 1.01$] as illustrated in Figure 16.

The monocline is flattened from $x = 0.50$ to $x = 0.60$ (i.e., $l = 0.10$). The slope to the left of the flattened interval is denoted h_a and to the right by h_b. In this interval $\Delta\gamma = -3.1°$, $\gamma(x_0) - 3.4°$, and Λ is large, as this is the region in which $q(x)$ has its largest gradients. (Its actual value is about 25%.) The con-

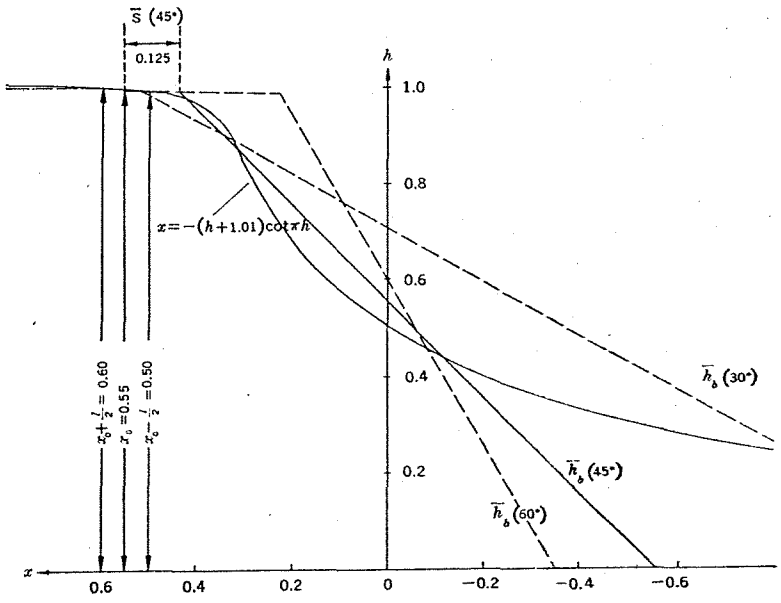

Fig. 16. Illustration of numerical example, section 7.

tribution of the slope term to the flattening error (equation 26) is $+0.01q(x_0)$, and the curvature term contributes $-0.015q(x_0)$. As we shall see, $q(x_0) \approx 0.5$, and hence the flattening error amounts to only a few tenths of 1% of the regional heat flow and can be neglected. The results for this case follow.

Exact solution:

$$\Delta q(x_0) = -0.58 \tag{27a}$$

Jeffreys approximation:

$$\Delta q'(x_0) = -0.675 \tag{27b}$$

$$\Delta q_b' = -0.69 \tag{27c}$$

$$\Delta q_a' = +0.015 \tag{27d}$$

From the discussion of the previous section

$$\Delta q_a \, \Delta q_a' = 0.015$$

The portion of the slope h_b near the station has an average slope of about 45°, and hence an approximating equivalent slope $\bar{h}_b$ is selected with an angle $\bar{\beta} = 45°$. From Figure 13

$$\Delta q_b \approx \overline{\Delta q_b} = \Delta q_b' + D(\beta = 45°, \Delta q' = -0.69) = -0.69 + 0.11 = -0.58$$

Substituting these values in (14) yields

$$\Delta q = 0.015 - 0.58 + (0.015)(0.58)[1 \pm 1]$$

$$\approx -0.57 \pm 0.01$$

This is to be compared with the exact result of -0.58 and contrasted with the Jeffreys approximation of -0.675. To obtain the above result it was not even necessary to determine the coordinate $\bar{s}$ of $\bar{h}$. However, it can readily be obtained from Figure 11, permitting $\bar{h}$ to be drawn on the cross section to verify the fit. From Figure 13 it is seen that near the brink the results are rather insensitive to the choice of $\bar{\beta}$; taking 30° or 60° would have raised or lowered the result by only 0.03. (Actually 60° is a β^* which must give a lower limit to Δq_b by (23).) It is clear from Figure 16 that $\bar{\beta} = 45°$ is the more reasonable choice.

8. VARIATION OF THE TOPOGRAPHIC ANOMALY WITH DEPTH

General relations. To this point the discussion has been concerned only with the flux of heat across the surface, i.e., with the limiting value of the thermal gradient at zero depth ($z = 0$). Even in oceanic measurements of geothermal flux, however, temperature gradients are determined from observations to finite depths (1 to 10 meters). It is necessary to determine the conditions under which topographic anomalies computed for the surface can be applied to gradients determined beneath it without appreciable error, i.e., conditions under which the gradient anomaly may be treated as superficial.

To investigate depth variations of heat flow analytically, we rewrite (3) in the form of (19).

$$\Delta q(x_0, z) = \frac{1}{\pi} \int_{-\infty}^{+\infty} \frac{h(x)[1 + e(x)]}{(x - x_0)^2} \Phi(\chi)\, dx \tag{28}$$

where

$$\chi = |x - x_0| z^{-1}$$
$$\Phi(\chi) = 1 - \chi^{-2}/(1 + \chi^{-2})^2 \tag{29}$$

Equation 28 is an exact expression for the effect of any two-dimensional topographic surface, $h(x)$, on the vertical gradient at the point (x_0, z). Although $e(x)$ is unknown, its physical interpretation is clear; it is the mean anomalous gradient in the relief at x.

Inspection of the form of the function Φ (Figure 17) and equation 28 points up a fundamental problem of attempting regionally meaningful measurements of thermal gradient at or near the surface. The function Φ greatly diminishes effects of topographic features whose horizontal distance from the station $(x - x_0)$ is not large relative to the depth of observation, i.e., relief for which χ is not large. It is just these features that can have a very great effect on the gradient at the surface because of the inverse square growth of the fraction in the integrand of (28). As z approaches the surface, Φ approaches unity for all x, and very small features very close to the station can have very large effects on the gradients.

The following results can be obtained from equation 28 (*TDT*, section 9):

I. *All topography of one sign: General* [$h(x) \geq 0$ *or* $h(x) \leq 0$, $\infty > x > -\infty$]. In this case

$$|\Delta q(x_0, 0)| > |\Delta q(x_0, z)| \qquad z > 0 \tag{30}$$

which can be stated as a theorem: *If the topographic relief is of one sign at the station (x_0) the heat-flow anomaly caused by this relief at (x_0, z) attains its greatest magnitude at the surface $z = 0$.*

The theorem applies to the Jeffreys approximation as well as to the exact result. However, it does not apply in general to the discrepancy $[D(x_0,z)]$ between the two. Hence it is quite possible for the error in the Jeffreys approximation to be greater at depth than at the surface. It can be shown that the theorem applies also to the transient case if the change of $h(x)$ with time is of the same sign as h (or is zero).

II. *Relief is of one sign and lies farther from the station than the depth of measurement.* $[h(x) = 0, |x - x_0| < z; h(x) \geq 0$ *or* $h(x) \leq 0, |x - x_0| > z]$. If the closest point of the relief to the station is at x_1 and

$$\chi_1 = |x_1 - x_0|/z \geq 1$$

then

$$\frac{\Delta q(x_0, z)}{\Delta q(x_0, 0)} > \Phi(\chi_1) \tag{31}$$

$$\frac{\delta q(x_0, z)}{\Delta q(x_0, 0)} > \Psi(\chi_1) \tag{32}$$

where $\delta q(x_0, z)$ represents the heat flow computed from two temperature measurements, one at the surface and the other at depth z, and

$$\Psi(\chi) = 2\chi \tan^{-1} \frac{1}{\chi} - 1 \tag{33}$$

It is shown with $\Phi(x)$ (equation 29) in Figure 17.

III. If relief is of one sign and is distributed throughout the region $|x - x_0| < 2z$, then $\Delta q(x_0, z)$ is generally an order of magnitude less than $\Delta q(x_0, 0)$.

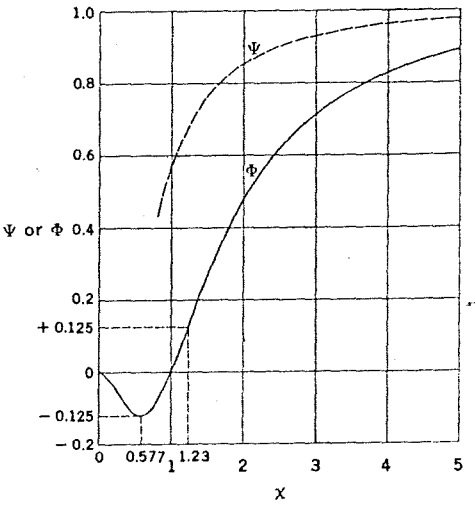

Fig. 17. The factors, Φ and Ψ, for depth dependence of the integrand in expressions for the gradient anomaly.

IV. It can also be shown that (*a*) if the relief is of both signs and lies in the region $|x - x_0| > z$, then $|\Delta q(x_0, z)|$ is less than the magnitude of the contribution of the positive or negative portion considered individually, whichever is larger, and (*b*) if the relief is of both signs and distribution is unrestricted, $|\Delta q(x_0, z)|$ is less than the sum of the magnitudes of the contribution of the positive and negative portions considered individually.

Discussion. From Figure 17 it is seen that

$$\Phi(\chi) > 0.89, \quad \chi > 5 \tag{34}$$

$$\Psi(\chi) > 0.86, \quad \chi > 2 \tag{35}$$

Hence, by II*a* and II*b* and IV*a*, for most purposes the gradient anomaly at depth z can be considered superficial if the closest significant relief is at a horizontal distance greater than $5z$; the mean gradient anomaly to depth z is superficial if the closest relief is at a distance greater than $2z$. (The latter case applies to suboceanic gradients based on a temperature measurement in the bottom water and one measurement in the sediment or to continental gradients determined from mean annual air temperature and bottom-hole temperature.) Inasmuch as the discrepancies referred to in II are relative ones, the height of the topography does not enter.

To put these results in perspective it is worth considering four cases:

(1) The gradient measurement is superficial and the height of the relief is greater than its distance from the station. In this case the present theory applies, but the Jeffreys approximation is uncertain.

(2) The measurement is superficial and the height does not exceed the distance from the station. Here the Jeffreys approximation generally applies, but the present method may still be used for convenience.

(3) The gradient measurement is not superficial but the height does not exceed the distance to the station. The present theory does not apply (except for limits imposed by I and III), but the Jeffreys approximation generally does.

(4) The measurement is not superficial and the height is larger than the distance to the station. This represents a trouble spot for the Jeffreys approximation not covered by the present theory (except for limits imposed by I and III).

Although the present methods can be convenient for rapid estimates in cases 1 and 2, it is only in case 1 that they provide information not obtainable from the Jeffreys approximation. Where continental measurements can be considered superficial, the application often falls under case 2 because the measurement depth is commonly of the same order as the relief.

Thus steady-state topographic corrections throughout a 300-meter borehole can be computed from solutions that are valid at the surface if the (two-dimensional) topographic relief is more than a kilometer or two from the station. Under such circumstances the Jeffreys approximation and the exact solution would give comparable results (case 2) unless the relief was very great (case 1). The topographic anomaly in the upper 30 meters of the hole could, of course, be considered superficial for relief extending to within 100–200 meters. For

relief of one sign at any distance, the surface correction will provide an upper limit.

Several problems associated with oceanic observations fall under case 1 because of the small depth of measurement.

Ocean-bottom heat-flow measurements. It is well known that oceanic heat-flow values often show considerable variation and that in most areas the spacing of the measurements is inadequate for a determination of the lateral scale over which these variations occur. Without such information it is difficult to determine the cause of the variation.

Inasmuch as relief is unknown in detail near an oceanic heat-flow station (with uncertainties of the order of meters to hundreds of meters, *TDT*, section 9), many workers have considered the effects of undetected relief as a possible source of these variations [e.g., *Bullard et al.*, 1956; *Langseth et al.*, 1966; *Lachenbruch and Marshall*, 1966; *Birch*, 1967].

The problem can be investigated by considering the theoretical effects of credible two-dimensional models of undetected relief. (The two-dimensional case is intermediate between the various three-dimensional possibilities; in the worst case, three-dimensional topography could produce anomalies that might exceed the corresponding two-dimensional ones by a factor of about 1½.) An upper limit to the scale of these models is imposed by the uncertainty δh in the determination of local elevation difference on the ocean floor. A lower limit to their scale is imposed by the length of the probe λ and the presence or absence of curvature in the temperature profile.

Suppose a temperature probe penetrates the ocean bottom at point x_0 (Figure 18) to depth λ and that local elevation differences are uncertain by $\pm\delta h$. According to III, if unseen relief is distributed within a distance 2λ of the station, it will generally produce a change in gradient over the length of the probe of the same order of magnitude as the mean gradient anomaly measured at the station. If such effects are large, they are easily identified with probes containing three or more sensors; if they are not large, they are unimportant. Relief beyond 2λ can produce

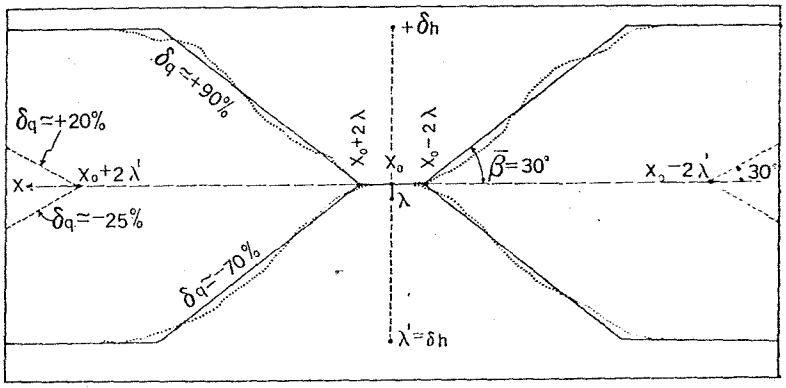

Fig. 18. Possible undetected relief ($\pm\delta h$) that would produce a superficial gradient disturbance to depth $\lambda = 0.1\delta h$ (solid lines) and $\lambda = \delta h$ (medium dashed lines).

anomalies in the mean gradient that are large relative to the curvature detectable with a few temperature sensors. Such unseen relief can have a height of $\pm\delta h$, and the worst case occurs when it is of the same sign on both sides of the station. Whatever the forms of these unseen slopes, they can be replaced by equivalent plane slopes of angle $\bar{\beta}$ at distance 2λ. The resulting anomaly (δq) can be considered superficial (35) and expressed approximately as

$$\delta q \approx 2\,\Delta\bar{q}(\bar{\beta},\, 2\lambda/\delta h) \tag{36}$$

The fraction represents r or s, depending on whether the relief is positive or negative. If it is very small, interaction should be considered (equations 10 or 11).

Because so little is known of small-scale sea-bottom topography, the choice of values for the height δh and mean slope $\bar{\beta}$ of unseen local slopes is an open question at present. Recent observations with deeply towed sounders have revealed relief on the order of 100 meters, with slopes as great as 30° [*Loughridge*, 1966; *Birch*, 1967] or even 45° to 90° [*Spiess et al.*, 1967]. Taking $\bar{\beta} = 30°$ and assuming the uncertainty δh is 10 times the probe penetration (λ), we find from (36) (modified by equations 10 and 11) that positive anomalies up to 90% and negative ones up to 70% could occur with relatively little curvature (Figure 18). If λ is 2 meters, this amounts to 20 meters of unseen relief. If the relief were 50 meters, the same anomalies could be caused by slopes beyond 5λ, and, by (34), no measurable curvature would occur.

Increasing the probe length by a factor of 10 (from $\lambda = 0.1\delta h$ to $\lambda' = \delta h$, Figure 18) decreases the limits of error (δq) to +20% and −25% plus a substantial fraction of the measured change in gradient with depth. In these examples the relief indicated by first arrivals on a conventional echo sounder would be of the order of 1 meter or less (*TDT*, section 9).

From (36) and Tables 1 and 2 it is seen that the probe length should be 2 or 3 times the elevation uncertainty, and the curvature should be negligible to reduce the topographic uncertainty to about ±10%. As these conditions are rarely fulfilled, the best assurance against undetected topographic anomalies is the agreement of closely spaced measurements [*Reitzel*, 1963; *Lister*, 1963; *Lee and Uyeda*, 1965; *Lachenbruch and Marshall*, 1966].

The lower limit of heat flow is approximately zero, and its upper limit is unrestricted. Hence we tend to view the frequency of occurrence of large heat-flow anomalies in the log-normal sense [*Girdler*, 1966]; a very low heat flow of one-fourth the regional average is an occurrence roughly comparable to a very high heat flow of 4 times the average, though the actual anomalies are −75% and +300%, respectively. In this sense, very low heat flows are much more easily explained by unseen relief than are very high ones, as the comparable high ones generally require elevation differences one or two orders of magnitude greater (Tables 1 and 2 and Figures 4 and 5). This observation is consistent with the recent discussion by *Birch* [1967].

9. TIME DEPENDENCE AND OTHER EFFECTS

Time dependence. Birch [1950] has shown that the finite times elasped during and since the evolution of topography can have appreciable effects on the

geothermal terrain correction. The present discussion concerns corrections to superficial gradient measurements, primarily a problem of accounting for close-in topography with short time constants. However, an approximate theory of the transient effect has been considered (*TDT*, section 10) to place the foregoing discussion in a time context.

Selected results are presented in Table 4 for unconsolidated sediments (thermal diffusivity $\alpha = 0.0025$ cm^2 sec^{-1}) and 'rock' ($\alpha = 0.0125$ cm^2 sec^{-1}). For topographic features whose height and distance are small relative to the sediment thickness, the value for sediment is probably more realistic. Larger, more distant features are probably represented better by the column headed 'rock.' In the table a feature should be considered as represented by its equivalent cliff.

From the second line we see that an open pit or mine dump made in this century would not affect the surface heat flow in a borehole only 100 meters away. By (30) the result applies to gradients throughout the borehole. More or less uniform relief approaching to within a kilometer or two of the station can be described by the equilibrium theory if the topography has not changed much since early Pliocene time and the sediments are thick—or early Pleistocene time if the sediments are thin. The latter case might apply, for example, to the walls of an oceanic trench for stations on the floor. A substantial fraction of the effect of slopes forming 10 m.y. ago would be felt at stations 5 or 10 km away. It is seen from the last column of Table 4 that effects of such slopes would generally be small.

Finite lapse rate. For convenience it has been assumed that the topographic surface is isothermal. If the temperature of the surface decreases linearly with elevation with gradient G', the topographic anomaly would be given by

$$[(G - G')/G]\,\Delta q \tag{37}$$

For terrain above sea level, approximations to G' are found to range from about 3 to 9°C/km. This is often 10 to 50% of G, and the topographic correction is substantially reduced. At abyssal depths in the ocean we normally have $G'/G \approx 10^{-3}$, as G' is of the order of the adiabatic gradient in sea water, and the assumption that the surface is isothermal is realistic.

A buried bedrock slope. Equation 37 suggests an additional application of the results presented in section 2. Suppose a bedrock surface dips under sedimentary material of conductivity K_1 and there is no topographic expression at the surface, as illustrated in Figure 19. If the conductivity of the rock is K, the gradient G_1 in the sediments at points distant from the slope is

$$G_1 = (K/K_1)G$$

As an approximation we assume that the gradient G_1 obtains throughout the sediment above the bedrock surface. Replacing G' by G_1 in (37) yields

$$\Delta q_b(x_0, \beta) \approx [1 - (K/K_1)]\,\Delta q(x_0, \beta) \tag{38}$$

where Δq_b is the heat-flow anomaly caused by the buried bedrock topography at points on the surface behind the brink (AB, Figure 19) and at the buried interface (BCD, Figure 18).

TABLE 4. Time in Years for Approach of Surface Heat Flow to Equilibrium after Generation of a Cliff at Distance x

Distance x, km	Equilibrium, %						$\Delta q(x)$ for 1-km cliff, $t = \infty$	
	90		50		10			
	Rock	Sediment	Rock	Sediment	Rock	Sediment	$\beta = +90°$ $(x = r)$	$\beta = -90°$ $(x = s)$
0.01	1.8×10^2	9.0×10^2	5.2	26	0.7	0.3	+2.9	−0.99
0.1	1.8×10^4	9.0×10^4	5.2×10^2	2.6×10^3	68	3.4×10^2	+0.86	−0.92
0.5	4.5×10^5	2.3×10^6	1.3×10^4	6.5×10^4	1.7×10^3	8.5×10^3	+0.32	−0.64
1.0	1.8×10^6	9.0×10^6	5.2×10^4	2.6×10^5	6.8×10^3	3.4×10^4	+0.20	−0.41
5.0	4.5×10^7	2.3×10^8	1.3×10^6	6.5×10^6	1.7×10^5	8.5×10^5	+0.05	−0.08
10	1.8×10^8	9.1×10^8	5.2×10^6	2.6×10^7	6.8×10^5	3.4×10^6	+0.03	−0.04
50	4.5×10^9	2.3×10^{10}	1.3×10^8	6.5×10^8	1.7×10^7	8.5×10^7	+0.006	−0.006

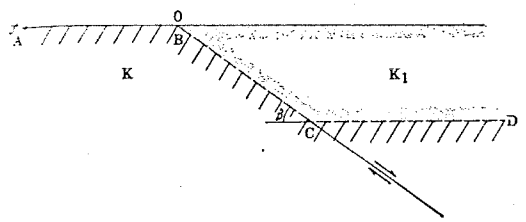

Fig. 19. Model of the down-faulted bedrock pediment.

If the conductivity of the bedrock is approximately twice that of the sediment (a common situation), the lower curves in Figure 3 give the negative of the anomaly along *AB* (Figure 19), and the upper curves of Figure 3 give the negative of the anomaly along the interface *CD* (Figure 19).

The model describes a common situation in the Basin and Range province of the western United States, where bedrock pediment surfaces are downfaulted on the basin side and the depression is subsequently filled with alluvium. The results are useful in the interpretation of geothermal data from boreholes in such areas.

Acknowledgments. I am grateful to J. H. Sass, W. H. K. Lee, and C. R. B. Lister for reading the manuscript and providing many useful suggestions. Roger Bowen and John Tanida provided invaluable assistance with numerical computation and programming.

This work is part of a continuing geothermal study by the U. S. Geological Survey. It is supported in part by the Office of Naval Research.

REFERENCES

Birch, Francis, Flow of heat in the Front Range, Colorado, *Bull. Geol. Soc. Am., 61,* 567–630, 1950.

Birch, Francis, Low values of oceanic heat flow, *J. Geophys. Res., 72*(8), 2261–2262, 1967.

Bullard, E. C., The disturbance of the temperature gradient in the earth's crust by inequalities of height, *Monthly Notices Roy. Astron. Soc., Geophys. Suppl., 4,* 360–362, 1938.

Bullard, E. C., A. E. Maxwell, and R. R. D. Revelle, Heat flow through the deep sea floor, *Advan. Geophys., 3,* 153–181, 1956.

Castoldi, Luigi, Sulla distribuzione della temperatura negli strati superiori della crosta terrestre [On the temperature distribution in the upper layers of the earth's crust], *Geofis. Pura Appl., 23,* 27–35, 1952.

Girdler, R. W., Statistical analyses of terrestrial heat flow observations (abstract), *Trans. Am. Geophys. Union, 47*(1), p. 182, 1966.

Jaeger, J. C., Application of the theory of heat conduction to geothermal measurements, in *Terrestrial Heat Flow, Geophys. Monograph 8,* edited by W. H. K. Lee, 7–23, American Geophysical Union, Washington, D. C., 1965.

Jaeger, J. C., and J. H. Sass, Lee's topographic correction in heat flow and the geothermal flux in Tasmania, *Geofis. Pura Appl., 54,* 53–63, 1963.

Jeffreys, Harold, The disturbance of the temperature gradient in the earth's crust by inequalities of height, *Monthly Notices Roy. Astron. Soc., Geophys. Suppl., 4,* 309–312, 1938.

Kober, H., *Dictionary of Conformal Representations,* 208 pp., Dover Publications, New York, 1952.

Lachenbruch, A. H., The effect of two-dimensional topography on superficial thermal gradients, *U. S. Geol. Surv. Bull., 1203-E,* in press, 1968.

Lachenbruch, A. H., and B. V Marshall, Heat flow through the Arctic Ocean floor: The Canada Basin-Alpha Rise boundary, *J. Geophys. Res., 71*(4), 1223–1248, 1966.

Langseth, M. G., Jr., Xavier Le Pichon, and Maurice Ewing, Crustal structure of the mid-ocean ridges, 5, Heat flow through the Atlantic Ocean floor and conviction currents, *J. Geophys. Res.*, *71*(22), 5321-5355, 1966.

Lee, W. H. K., and Seiya Uyeda, Review of heat flow data, in *Terrestrial Heat Flow, Geophys. Monograph 8*, edited by W. H. K. Lee, pp. 87–190, American Geophysical Union, Washington, D. C., 1965.

Lister, C. R. B., A close group of heat-flow stations, *J. Geophys. Res.*, *68*(19), 5569–5573, 1963.

Loughridge, M. S., Microrelief and magnetic anomalies of the sea floor off southern California (abstract), *Geol. Soc. Am., Ann. Meetings Program*, p. 126, 1966.

Reitzel, John, A region of uniform heat flow in the North Atlantic, *J. Geophys. Res.*, *68*(18), 5191–5196, 1963.

Spiess, F. N., B. P. Luyendyk, R. L. Larson, W. R. Normark, and J. D. Mudie, Detailed submarine geology of the deep-sea floor (abstract), *Trans. Am. Geophys. Union*, *48*(1), 134–135, 1967.

(Manuscript received November 30, 1967.)